Article

A Dynamical Key to the Riemann Hypothesis: Part I

Chris King*

Emeritus, Mathematics Department, University of Auckland

ABSTRACT

We investigate a dynamical basis for the Riemann hypothesis[1] (RH) that the non-trivial zeros of the Riemann zeta function lie on the critical line x = ½. In the process we graphically explore, in as rich a way as possible, the diversity of zeta and L-functions, to look for examples at the boundary between those with zeros on the critical line and otherwise. The approach provides a dynamical basis for why the various forms of zeta and L-function have their non-trivial zeros on the critical line. It suggests RH is an additional unprovable postulate of the number system, similar to the axiom of choice, arising from the asymptotic behavior of the primes as $n \to \infty$. Part I of this article includes: Introduction; The Impossible Coincidence; Primes and Mediants - Equivalents of RH; A Mode-Locking View of Dirichlet L-functions and their Counterexamples; Widening the Horizon to other types of Zeta and L-Function; L-functions of Elliptic Curves; and Modular and Automorphic Forms.

Key Words: dynamical key, Riemann Hypothesis, non-trivial zero, unprovable, asymptotic.

Introduction

The Riemann zeta function $\zeta(z) = \sum_{n=1}^{\infty} n^{-z} = \prod_{p\ prime} \left(1 - p^{-z}\right)^{-1}$ Re(z)>1 is defined as either a sum of complex exponentials over integers, or as a product over primes, due to Euler's prime sieving.

The zeta function is a unitary example of a Dirichlet series $\sum_{n=1}^{\infty} a_n n^{-z}$, which are similar to power series except that the terms are complex exponentials of integers, rather than being integer powers of a complex variable as with power series. We shall examine a variety of Dirichlet series to discover which, like zeta, have their non-real zeros on the critical line x = ½ and which don't.

In historical terms, there is a unique class of such series, which do appear to have their unreal zeros on the critical line - the Dirichlet *L*-series, or when extended to the complex plane, *L*-functions:

$$L(z,\chi) = \sum_{n=1}^{\infty} \chi(n) n^{-z} = \prod_{p\ prime} \left(1 - \chi(p) p^{-z}\right)^{-1}$$ where $\chi(n),\ n = 0,\ldots,k-1$ is a Dirichlet character.

* Correspondence: Chris King http://www.dhushara.com E-Mail: chris@sexualparadox.org
Note: This work was completed 11 May – 16 Oct 2011 .

[1] Links in blue which do not have an htm reference refer to Wikipedia search items, or in the case of Collatz conjecture, Mellin transform, prime counting and grand unitary ensemble to the live htm link in King 2009.

(The images in the figures are generated using a Mac software research application developed by the author, which is available at: http://dhushara.com/DarkHeart/RZV/. It includes open source files for XCode compilation for flexible research use and scripts for the open source math packages PARI-GP and SAGE to generate *L*-functions of elliptic curves and modular forms.)

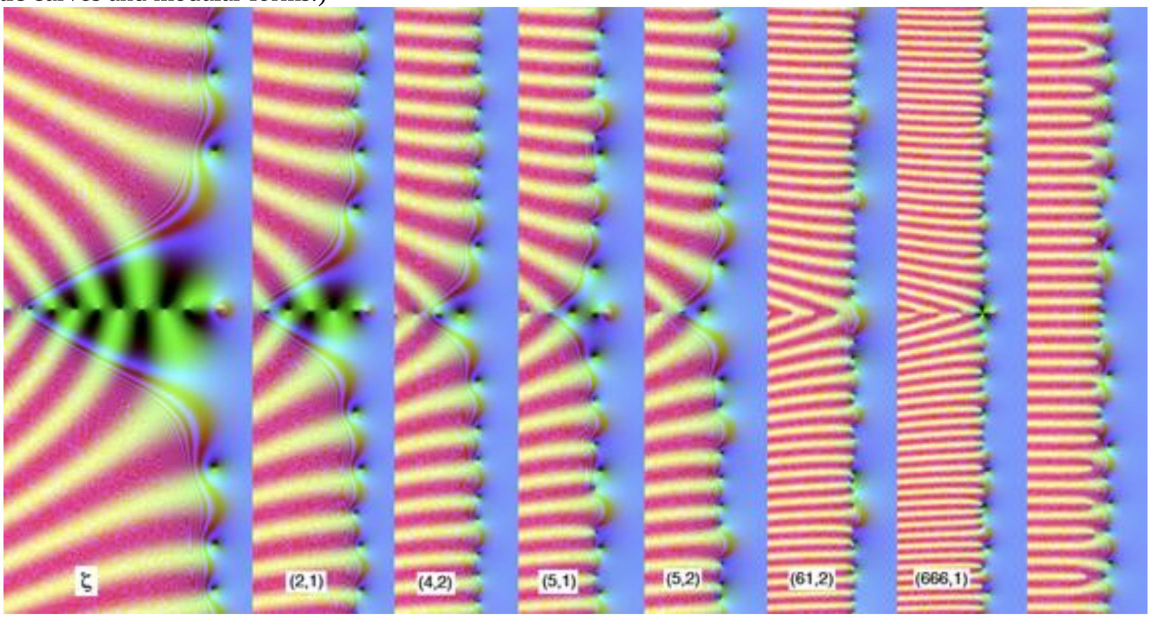

Fig 1: Riemann zeta and a selection of Dirichlet *L*-functions with a non-*L* function for comparison: *L*(2,1) and *L*(5,1) have regular zeros on $x = 0$ as well as non-trivial zeros on $x = ½$, due to their being equal to zeta with additional prime product terms. While *L*(4,2) is symmetric with real coefficients, *L*(5,2) and *L*(61,2) have asymmetric non-trivial zeros on $x = ½$, having conjugate *L*-functions. *L*(666,1) is similar to *L*(2,1) and *L*(5,1), but has a central third-order zero due to 666 being the product of three distinct primes $666=2.3^2.37$. Far right the period 10 non-*L*-function with $\chi = \{0,1,0,-1,0,0,0,1,0,-1\}$ (portrayed naked of any functional equation for 100 terms) has zeros in the critical strip $0<x<1$ manifestly varying from the critical line. Images generated using the author's application RZViewer for Mac (http://www.dhushara.com/DarkHeart/RZV/RZViewer.htm).

It was originally proven by Dirichlet that $L(1, \chi) \neq 0$ for all Dirichlet characters χ, allowing him to establish his theorem on primes in arithmetic progressions. While $\zeta(1)$ is singular, $L(1,\chi)$ for non-trivial characters is known to be transcendental (Gun et. al.). For example $1-\frac{1}{3}+\frac{1}{5}-\frac{1}{7}\ldots = L\left(1,\chi(4,2)\right)=\frac{\pi}{4}$, leading to the study of special values of *L*-functions.

A Dirichlet character is any function χ from the integers to the complex numbers, such that:
1) **Periodic:** There exists a positive integer k such that $\chi(n) = \chi(n + k)$ for all n.
2) **Relative primality:** If $\gcd(n,k) > 1$ then $\chi(n) = 0$; if $\gcd(n,k) = 1$ then $\chi(n) \neq 0$.
3) **Completely multiplicative:** $\chi(mn) = \chi(m)\chi(n)$ for all integers m and n.

Consequently $\chi(1)=1$ and since only numbers relatively prime to k have non-zero characters, there are $\phi(k)$ of these where ϕ is the totient function, consisting of the number integers less than n coprime to n, and each non-zero character is a ϕ-th complex root of unity. These conditions lead to the possible characters being determined by the finite commutative groups of units in the quotient ring Z/kZ, the residue class of an integer n being the set of all integers congruent to n modulo k.

As a consequence of the particular definition of each χ, $L(z, \chi)$ is also expressible as a product over a set of primes p_i with terms depending on the Dirichlet characters of p_i. As well as admitting an Euler product, oth Riemann zeta and the Dirichlet *L*-functions (*DL*-functions) also have a generic functional equation enabling them to be extended to the entire complex plane minus a simple infinity at $z = 1$ for the principal characters, whose non-zero terms are 1, as is the case of zeta.

Extending RH to the *L*-functions gives rise to the generalized Riemann hypothesis - that for all such functions, all zeros on the critical strip $0 < x < 1$ lie on $x = ½$. Examining where the functional boundaries lie, beyond which the unreal zeros depart from the critical line, has become one major avenue of attempting to prove or disprove RH, as noted in Brian Conrey's (2003) review. Some of these involve considering wider classes of functions such as the *L*-functions associated with cubic curves, echoing Andre Weil's (1948) proving of RH for zeta-functions of (quadratic) function fields. Here, partly responding to Brian Conrey's claim of a conspiracy among abstract *L*-functions, we will restrict ourselves to the generalized RH in the standard complex function setting, to elucidate dynamic principles using Dirichlet series inside and outside the *L*-function framework.

The Impossible Coincidence

To ensure convergence, zeta is expressed in terms of Dirichlet's eta function on the critical strip: $\zeta(z) = \left(1-2^{1-z}\right)^{-1} \sum_{n=1}^{\infty} (-1)^{n+1} n^{-z} = \left(1-2^{1-z}\right)^{-1} \eta(z)$ and then in terms of the functional equation $\zeta(z) = 2^z \pi^{-1+z} \sin\left(\frac{\pi z}{2}\right) \Gamma(1-z)\zeta(1-z)$ where $\Gamma(z) = \int_0^{\infty} t^{z-1} e^{-t} dt$ in the half-plane real(z)≤0.

In terms of investigating the convergence of the series to its zeros, eta is better placed than zeta because the convergence is more uniform, as shown in fig 2.

RH is so appealing, as an object of possible proof, because of the obvious symmetry in all the zeroes lying on the same straight line, reinforced by Riemann's reflectivity relation:

$$\Gamma\left(\frac{z}{2}\right) \pi^{-\frac{z}{2}} \zeta(z) = \Gamma\left(1-\frac{z}{2}\right) \pi^{-\frac{1-z}{2}} \zeta(1-z)$$

making it possible to express the zeros in terms of the function xi: $\xi(z) = \frac{1}{2} z(z-1) \Gamma\left(\frac{z}{2}\right) \pi^{-\frac{z}{2}} \zeta(z)$ for which $\xi(z) = \xi(1-z)$, so it is symmetric about $x = ½$, leading to any off-critical zeros of zeta being in symmetrical pairs. The function $\Xi(z) = \Gamma\left(\frac{z}{2}\right) \pi^{-\frac{z}{2}} \zeta(z)$ also has this symmetry. It also applies to the *L*-functions, for which: $\xi(z,\chi) = \Gamma\left(\frac{z+a}{2}\right) (\pi/q)^{-\frac{z+a}{2}} L(z,\chi),\ a = \{\chi(-1) \equiv -1\}$, with $i^a k^{1/2} \xi(z,\chi) = \sum_{n=1}^{k} \chi(n) e^{2\pi n i/k} \xi(1-z,\overline{\chi})$.

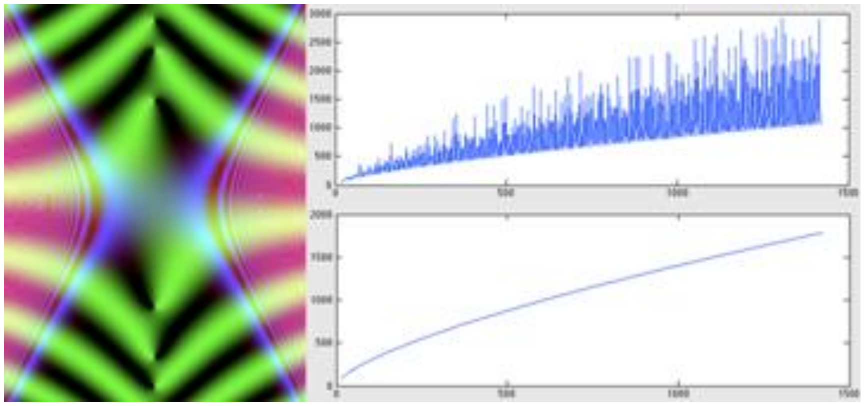

Fig 2 (Left) Symmetry in xi means any off-critical zeros have to be in symmetric pairs. (Top) The number of iteration steps in the eta-derived zeta series required to get 5 steps with 0.005 of 0 varies erratically from one zero to the next, but this is a disguised effect of the presence of the $1/(1-2^{1-z})$ term so becomes a smooth curve for eta (below).

However, when we come to examine the convergence in detail, this symmetry seems to be lost in the actual convergence process. Each term in the series for zeta is $n^{-x+iy} = n^{-x}(\cos(y\ln n) + i\sin(y\ln n))$, forming a series of superimposed logarithmic waves of wavelength $\lambda = \dfrac{2\pi}{\ln n}$, with the amplitude varying with $n^{-1/2}$ for points on the critical line. Unlike power series, which generally have coefficients tending to zero, Dirichlet *L*-functions have coefficients all of absolute value 1, which means all the wave functions are contributing in equal amplitude in the sum except for the fact that the real part forms an index determining the absolute convergence. So RH is equivalent to all the zeros being at the same real (absolute) address.

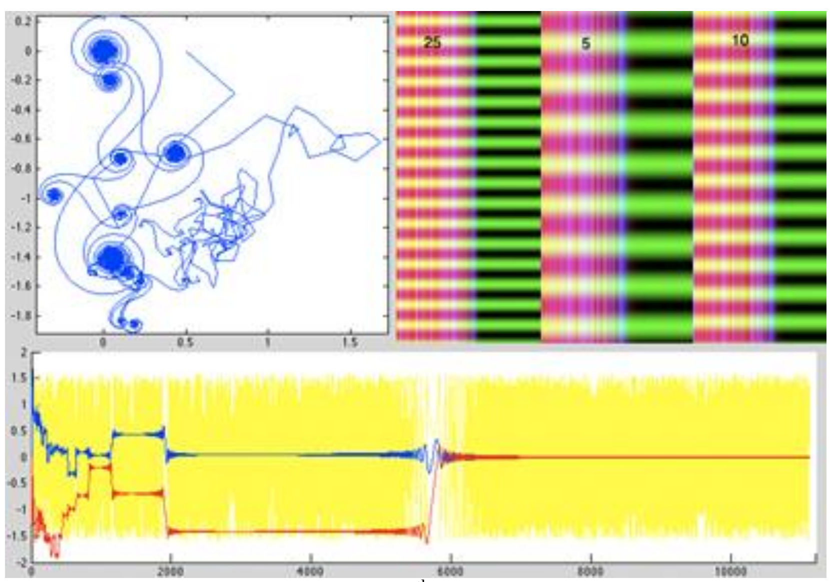

Fig 3: Top left sequence of iterates of eta for the 20,000th zero, showing winding into and out of a succession of spirals linking the real and imaginary parts of the iterates. Top right: The wave functions are logarithmic, leading to powers, but not multiples, having harmonic relationships. Below is shown the real and imaginary parts of the iterates (blue and red) overlaid on the phase angle of individual terms (yellow). The zero is arrived at only after a long series of windings interrupted by short phases of mode-locking in the phases of successive terms.

The logarithmic variation means that the wave functions are harmonic only in powers, e.g. 5, 25, 125 etc. and not in multiples. There is no manifest relationship between ln *n* and $n^{1/2}$ that explains why the zeros should be on *x* = ½ and indeed we will find examples where they are not, so there is another factor involved - the primes. Powers of primes or their negation are reflected in both Riemann's primality proofs and other functions, such as the Möbius function:

$$\frac{1}{\zeta(z)}=\sum_{n=1}^{\infty}\frac{\mu(n)}{n^z},\ \mu(n)=\begin{cases}(-1)^k, & n \text{ has } k \text{ distinct prime factors of multiplicity } 1\\ 0 & \text{otherwise}\end{cases}.$$

The iterative dynamics give an immediate clue to the potential uncomputability of this problem. If we take a given zero of eta, say the 20,000th, and plot the iterates, we find successive *n*-term approximations wind into and out of a series of spirals associated with non-phase locked epochs, where the angle of successive terms is rotating steadily, interrupted by briefer periods of phase locking, where the angles remain transiently static and hence the complex values of the iteration make a systematic translation. Eventual convergence to zero or another final value occurs only after the last of these mode-locking episodes (see appendix 1) , whose iteration numbers can be calculated directly, by finding where the waves match phase:

$$y\ln(n+1)=y\ln(n)+k\pi \Leftrightarrow \ln\left(\frac{n+1}{n}\right)=\frac{k\pi}{y}\Leftrightarrow 1+\frac{1}{n}=e^{k\pi/y}\Leftrightarrow n=\frac{1}{e^{k\pi/y}-1}.$$

This corresponds also to the mode shifts in the phase-locking of the orbits in yellow in fig 3. Between the phase locked translations, the iterative value winds towards and then away from an equilibrium value because the angular rotation tends to periodically cancel the effects of intervening terms. After the last phase-translation, further terms simply cause asymptotic convergence to the equilibrium. These effects are all caused because we are dealing with a discrete sum $\sum_{n=1}^{\infty}a(n)n^{-z}$, rather than the continuous integral, which in the case of zeta would simply be polynomial integral $\int_0^{\infty}t^{-z}dt$. It is the transient discrete effects of the phase-locked translations, which determine the eventual value of any Dirichlet series at a given point, so effectively we have a discrete computational problem for each potential zero over the integers, at least up to the last phase translation. This suggests that although the zeros of zeta and the *L*-functions lie hovering temptingly on the critical line, their location can be determined within ε only by explicit computation over the sequence of terms, suggesting RH is a potentially unprovable problem of non-inductive integer computation just as simpler unproven conjectures such as the Collatz conjecture are, although palpably true in each finite case (King 2009).

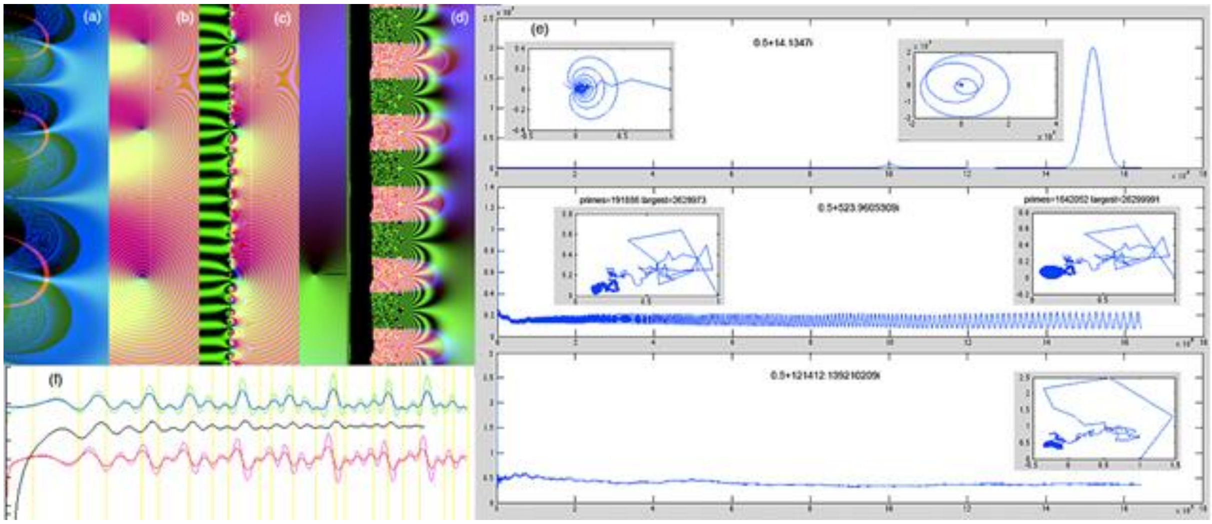

Fig 4 (a) X-ray view of zeta with curves of Re(ζ)=0 (red) and Im(ζ)=0 (cyan) show neither alone determines the location of the zeros. (b,c) log(abs(1/(1-ζ)) plot of the analytic and product forms of zeta show their divergence for $x<1$ and identity for $x>1$. (d) Large fluctuation at the first zeta zero for the product of 84270 primes due to the (red) tongue moving across the zero as the number of product terms increases. (e) Iterative dynamics of the product are radically unstable, leading eventually to exponentiating fluctuations even at the zeros, but these take an extreme number of primes to appear for higher zeros. (f) Fluctuations of real (blue,green) and imaginary (red,magenta) parts of zeta along $x=1$ approximate those of $x=1/2$, the zeros (yellow), and the Fourier sin transform (black) of an integer step function.

It is difficult to apply the Euler product directly to the zeros because it is radically non-convergent in the critical strip and equality with the Dirichlet series holds only for $x>1$ and although variations in values along the line $x=1$ where the sum and product formulations are equivalent do approximate the real and imaginary fluctuations along the critical line.

In fig 4 are shown some of the dynamic features of the Euler product of zeta in comparison with the analytic Dirichlet sum. The sum and product representations diverge in the half plane $x<1$ while being identical on $x>1$. In the critical strip, the iterated product has radical divergence with orbits at the zeros first erratically fractal before setting into exponentiating pulses of divergence, as tongues of large value move down the strip with escalating prime values. When we evaluate the cumulative product up to the 1,642,052th prime 26299991, we find the first zero y~14 (top) has grown to a peak of around 10 million, while the zero y~523 (middle) has only begun to enter its first oscillatory burst around the 200,000th prime of around 3 million and y~121412 is as yet showing no signs of having fully explored its fractal dynamics

However zeta values along $x=1$ do fluctuate in a way which approximates both the imaginary values of the zeros and a Fourier sin transform of an integer step function (the corresponding prime transform also reflects the zeta zeros - see Conrey), showing the distribution of the zeros is transform-based, as demonstrated in Riemann's original proof.

Generally the existence of an Euler product formulation for the sum is seen as a pre-condition for well-behaved *L*-functions and a way of generating new types of *L*-function through prime mediated generators such as elliptic curves which form Euler products determining sum coefficients through prime factorization, which also possess a functional equation representation in the left-half plane.

Primes and Mediants - Equivalents of RH

Riemann developed an explicit formula for the prime counting function $\pi(x)$ which is most easily expressed in terms of the related prime counting step function $\psi(x)=\sum_{n\le x}\Lambda(x)$, the additive von Mangoldt function, where $\Lambda(x)=\log p$ if $x=p^k$ and 0 otherwise. Notice here the exclusive appearance of prime powers eliminated in the Möbius function. We then have the explicit formula $\psi(x)=x-\sum_{\substack{\zeta(\rho)=0\\ 0<\mathrm{Re}(\rho)<1}}\frac{x^\rho}{\rho}-\frac{1}{2}\log\left(1-x^{-2}\right)-\log(2\pi)$, where $\rho=1/2+it$ are the zeros of $\zeta(z)$, and the summation is over zeros of increasing $|t|$.

From Ingham (1932 83), we have $\pi(x)=\mathrm{li}(x)+O(x^\theta\ln x)$ where $\theta=\sup_{\rho:\zeta(\rho)=0}(real(\rho))$, $\mathrm{li}\,x=\int_0^x\frac{dt}{\ln t}$. Hence the asymptotic behavior of the primes is determined by the real sup of the zeros. This comes about because the explicit formula shows the magnitude of the oscillations of primes around their expected position is controlled by the real parts of the zeros of the zeta function, since

$$\frac{x^\rho}{\rho}=\frac{e^{(p+iq)\ln(x)}}{p+iq}=\frac{x^p(\cos(q\ln x)+i\sin(q\ln x))}{p+iq}=\frac{x^p}{p^2+q^2}(\cos(q\ln x)+i\sin(q\ln x))(p-iq)$$

$$\text{so }\frac{x^\rho}{\rho}+\frac{x^{\bar\rho}}{\bar\rho}=2\,\mathrm{real}\left(\frac{x^\rho}{\rho}\right)=2\frac{x^p}{p^2+q^2}(p\cos(q\ln x))+q\sin(q\ln x))\sim 2\frac{x^p}{p^2+q^2}q\sin(\ln(x)q).$$

Hence RH has been shown to be equivalent to the statement $|\pi(x)-li(x)|<x^{1/2}\log(x)/8\pi$.

A further equivalent of RH is that $M(x)=\sum_{n\le x}\mu(n)=O(x^{1/2+\varepsilon})$, which would guarantee the Möbius function would converge for x > ½, and show there were no infinite poles (and hence no zeta zeros). Likewise we have

$\sum_{n\le x}\lambda(n)=O(x^{1/2+\varepsilon}),\ \lambda(n)=(-1)^{\Omega(n)},\ \Omega(n)=$ no prime factors with multiplicity, the Liouville function.

Even more basic functional approximations have been found using the floor function (Cloitre).

However Mertens conjecture that $\mathrm{M}(n)=\sum_{k=1}^{n}\mu(k)<n^{1/2}$, which would have proved the Riemann hypothesis, was found false at a value of around 10^{30} by Odlyzko and Herman te Riele (1985), who also showed that $\pi(x)<\mathrm{li}(x)$ fails for some unspecified x < 6.69 x 10^{370}. Even more unachievable potential anomalies arise from considering the number of zeta zeros up to T:

$$N(T)=\frac{T}{2\pi}\log\left(\frac{T}{2\pi}\right)-\frac{T}{2\pi}+\frac{7}{8}+S(T)+O\left(\frac{1}{T}\right),\ S(T)=\frac{1}{\pi}\arg\zeta\left(\frac{1}{2}+iT\right)=O(\log T).$$

If RH is true we have a much closer bound $S(T) = O\left(\frac{\log(T)}{\log(\log(T))}\right)$ (Ivic). Odlyzko (1992) showed that $S(T)/(\log(\log(T))^{1/2}$ resembles a Gaussian random variable with mean 0 and variance $2\pi^2$, which means it is occasionally much larger than $(\log(\log(T))^{1/2}$. These results suggest we may only see asymptotic behavior when $|S(T)|$ reaches beyond current limits of around 3.2 (Odlyzko 2002) to values such as 100, implying $T \sim 10^{10^{100}}$, beyond reach of current computational methods.

The Farey sequences appear in a third manifestation of RH (Franel and Landau 1924). These consist of all fractions with denominators up to *n* ranked in order of magnitude - for example, $F_5 = \left\{\frac{0}{1}, \frac{1}{5}, \frac{1}{4,}, \frac{1}{3}, \frac{2}{5}, \frac{1}{2}, \frac{3}{5}, \frac{2}{3}, \frac{3}{4}, \frac{4}{5}, \frac{1}{1}\right\}$. Each fraction is the mediant (see appendix 1) of its neighbours (i.e. $\frac{n_1+n_2}{d_1+d_2}$). For an adjacent pair $\frac{a}{b}, \frac{c}{d}, bc - ad = 1$. Because the sequence of fractions removes degenerate common factors from the numerator and denominator, they are relatively prime and hence $|F_n| = |F_{n-1}| + \varphi(n)$ since F_n contains F_{n-1} plus all fractions $\frac{p}{n}$ where *p* is coprime to *n.*

Two Farey sequence equivalents of RH state:

$$\text{(i)} \sum_{k=1}^{m_n} |d_{k,n}| = \mathrm{O}\left(n^r\right), \text{ any } r > 1/2 \text{ and (ii)} \sum_{k=1}^{m_n} d_{k,n}^2 = \mathrm{O}\left(n^r\right), \text{ any } r > -1$$

$$d_{k,n} = a_{k,n}, -\frac{k}{m_n}, \text{ where } m_n \text{ is the length of the Farey sequence } \left\{a_{k,n},\ k = 1,\ldots,m_n\right\}$$

This is saying that the **Farey fractions are as evenly distributed as they can be** (to order $n^{1/2}$) **given that they are by definition not evenly distributed [1]**, but determined by fractions with all (prime) common factors removed.

The same consideration applies to the asymptotic **distribution of the primes** - **they are as evenly distributed as they can be** (to order $n^{1/2}$ from li(n)) - **given that they are not evenly distributed [2]**, being those integers with no other factors.

This is reflected in other properties of the prime distribution, despite its manifest irregularity, in such processes as the quadratic Ulam spiral. For example, the Dirichlet prime number theorem, states that there are infinitely many primes which are congruent to *a* modulo *d* in the arithmetic progression *a*+*nd*. Stronger forms of Dirichlet's theorem state that different arithmetic progressions with the same modulus have approximately the same proportions of primes. Equivalently, the primes are evenly distributed (asymptotically) among each congruence class modulo *d*.

What RH - that **the non-trivial zeros of the zeta function are all on the critical line [3] -** shows us is the order to which these fluctuations approach an even distribution is inverse quadratic because all the zeros appear to lie on x = ½. However the lack of a proof of RH suggests that these three statements are encoded forms of one another and that the locations of the zeros are a **consequence** of the distribution of primes rather than proving their asymptotic distribution, or at best that the three statements are encoded versions of one another. Thus RH is either true but unprovable except in finite numerical approximations, or a type of additional axiom like the axiom of choice that arises from infinities in calculation, just as the Collatz, and other discrete infinity problems appear to be versions of the undecidable Turing halting problem. Turing himself tried to prove computationally that RH was false! (Booker 2006).

We now turn to examining how a dynamical interpretation of the zeta zeros can explain why zeta and the Dirichlet *L*-functions have their non-trivial zeros on the critical line as a result of the asymptotically even distribution of the primes avoiding mode-locking which could knock the zeros ‘off-line’, as is the case for related functions where mode-locking is more pronounced.

A Mode-Locking View of Dirichlet *L*-functions and their Counterexamples

When we look at the sum formula for zeta, it appears to be simply a sum of powers of integers without the primes we see in the product formula, however, immediately we turn to zeta variants such as $\frac{1}{\zeta(s)} = \sum_{n=1}^{\infty} \frac{\mu(n)}{n^s}$ and $\frac{\zeta'(s)}{\zeta(s)} = -\sum_{n=1}^{\infty} \frac{\Lambda(n)}{n^s}$, we see the primes reappearing the coefficients.

In the context of the natural numbers, the minimally mode-locked numbers are the primes, since the only common factor of a prime with any other number, apart from itself, is 1. If we turn to the *L*-functions, we see their characters are constructed to eliminate any form of mode locking in three distinct ways, while keeping all the non-zero contributions to the superimposed wave function of equal unit weight:

(1) All coefficients of the bases not relatively prime to the period k are set to zero, leaving $m = \phi(k)$ relatively prime coefficients.

(2) The remaining coefficients of the relatively-prime bases are distributed cyclically with equally weighted values of absolute value 1 in the m-th roots of unity, according to a power of a generator of the m units of Z/Zk.

(3) Since the group generators result in a sum that can also be represented as a product function over primes, the asymptotic distribution of primes places a final limit on any phase-locking.

The negation of the non-relatively prime bases is consistent with the removal of one or more series $\sum_{n=1}^{\infty} (\pm 1)^{n-1} (qn)^{-z}$, $q \setminus k$, for which RH applies, but the distribution around the relatively prime residues with rotating coefficients arises from the group generators and the product representation, which again shows the primes becoming evident in the sum formula. Thus although periodic solutions might appear to be mode-locked these periodic solutions are the least mode-locked coefficient series in terms of integrating in an equi-distributed way with the prime distribution.

These conditions have been abstractly generalized into the four axioms of the Selberg class, attempting to define the conditions causing a Dirichlet series $L(z)$ to have zeros on the critical line: (1) Functional equation and (2) Euler product

(3) Coefficients of order 1. Ramanujan conjecture $a_1 = 1,\ a_n = n^{\varepsilon}\ \forall \varepsilon > 0$.

(4) At most a single simple pole infinity at 1 i.e. $(z-1)^m L(z)$ analytic for some m.

Pivotally the existence of an Euler product is a signature of non-mode-locking because, in a product structure, each of the factors are acting independently with no feedback between them. We shall firstly look generally at Dirichlet series and then focus firstly on L-functions that do have both a product structure and a functional equation and then on other variants that arise from products. In abstract L-functions, the form of the functional equation varies discretely, with a finite number of gamma factors dependent on the underlying topology of the prime process generating the product. The Ramanujan conjecture separates functions with weight 1 from different weightings which have non-trivial zeros on a different critical line (see later).

To assess the status of RH, we thus consider a wider class of Dirichlet series functions, to explore the effects of mode-locking of the wave functions in the critical strip. As a starting point we look at series where the coefficients are all 0 or roots of unity, but do not satisfy L-function conditions. The only Dirichlet L-function solutions from the finite group theory are periodic, the period kn consisting of characters in k that are perfect periodic repeats of k characters and not cyclic, or fractal permutations. Non-primitive characters are likewise generated from homologies of the residue groups $\chi_{kn}(p) = \chi_k(p \bmod k),\ \chi_{kn}(p) \neq 0$. Key here is the requirement for complete multiplicativity arising from the Euler product, each integer being a unique product of primes.

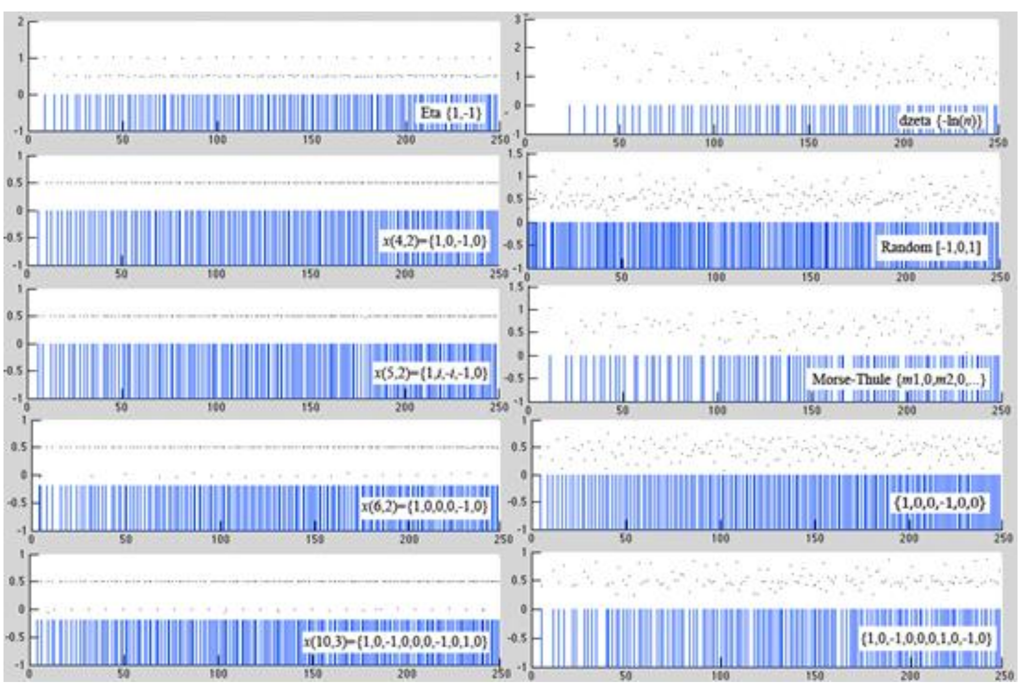

Fig 5: A series of L-functions and Eta (left) and RH-violating Dirichlet functions (right) whose critical strip zeros are illustrated by plotting their location (above) and their cumulative frequency, using a Matlab Newton's method scan.

In fig 5 on the left are shown the zeros of eta and a set of typical *L*-functions, confirming both the confinement of the zeros on $0 < x < 1$ to x = ½, and the $t.\ln(t)$ related cumulative frequency, discovered in Riemann's analysis of the zeta zeros. The method looks along a series of closely-spaced values running vertically for local absolute minima and then performs Newton's method using the approximate formal derivative for small *h*. On the right are shown a series of greater and lesser violations of the *L*-function / Selburg class conditions. Note that the derivative of zeta, despite not having an Euler product, does inherit a functional equation from zeta and its zeros are wide of the critical line, implying the functional equation is by no means sufficient, although it does define a symmetry about the critical line. Further examples are the Hurwitz and Davenport-Heilbron zeta functions (see later).

From the top down we have the derivative of zeta $\zeta'(z)$ by formal differentiation of the functional equation, which has terms effectively growing with -ln(*n*). Its zeros, corresponding to critical points of zeta, extend far out of the critical strip with an average real part of over 1. The next are Dirichlet series of random equi-distributed integers from {-1, 0 and 1}. This shows zeros distributed with means close to x = ½. Morse-Thule is a fractal sequence with even coefficients zero and the vector of odd coefficients recursively generated by v = [v, –v] with initial condition v = 1 viz {1,-1,-1,1,-1,1,1,-1 …} Again this has a mean close to x = ½.

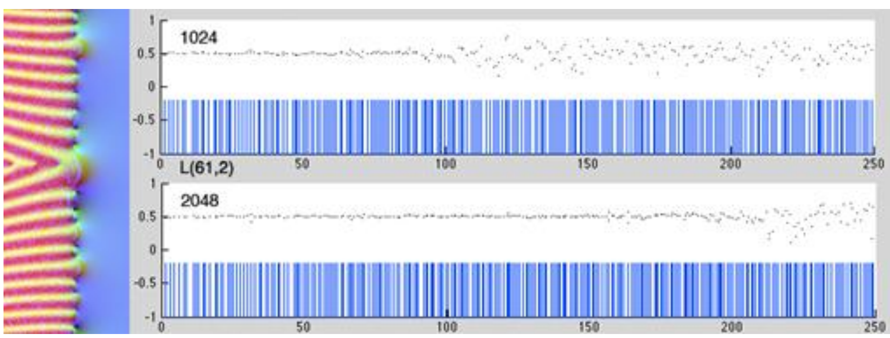

Fig 6: Even with a confirmed *L*-function such as Dirichlet *L*(61,2) higher periods cause delayed convergence, requiring a disproportionate number of function terms to recognize zeros tending to the critical line.

The last two are variants of the *L*-functions on their left by minor substitution. The first is effectively an alternating arithmetic series in 3's similar to that in 2's of χ (4,2), namely $1^{-z} - 4^{-z} + 7^{-z} - \ldots$, showing arithmetic series of bases appear to have zeros on the critical line if and only if they correspond to *DL*-functions. In particular, these modified series are not necessarily completely multiplicative, as all *L*-functions are leading to them not having a straightforward expression as an Euler product of primes. This may itself be sufficient reason for the non-*L* functions to be off-critical.

Function	**Means over zeros** in [0,1000]
Dzeta	1.1174
Random [-1,0,1]	0.5306, 0.4891, 0.4905
Morse-Thule ±{0,+/-1,0,-/+1}	0.5161
Golden Angle Rotation	0.6290
{1,0,0,-1,0,0}	0.4761
{1,0,-1,0,0,0,1,0,-1,0}	0.4959

Table 1: Some average *x* coordinates in the critical strip

From table 1 we can also see that, although these variants may have neither a functional equation nor an exact symmetry around the line $x = ½$, the mean real value of their zeros still lie close to the critical line. This is also consistent with the average trends in zeta functions. For example, if we take the curve $f(x) = 1 - \underset{y=20...120 \text{ step } 0.01}{\text{geometric mean}}(abs(\zeta(x+iy)-1))$, we find it has a zero at ~0.5646, reflecting the innate symmetry of the xi function of fig 2.

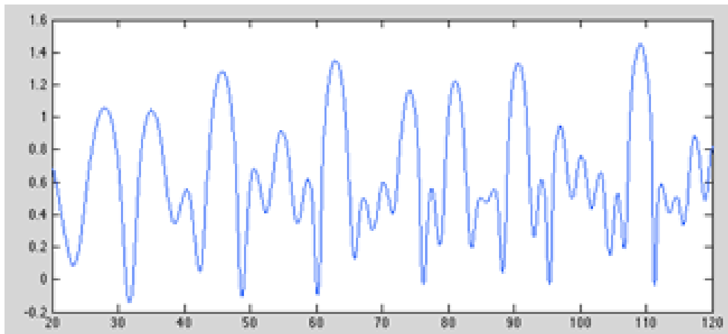

Fig 7: Function $p(y)$ showing the x-coordinate for each y, where the absolute value of zeta differs by 1 from 1.

Alternatively when we take the individual curve $p(y) = \{x : |\zeta(x+iy)-1| = 1\}$ in the interval [20,120], as in fig 7, we find it has a geometric mean of 0.4965.

While these estimates are just very rough ad-hoc approximations because of the exponentiating irregularity of all these functions, they do indicate how zeros of Dirichlet functions can deviate significantly from the critical line while still having an averaged behavior closely spanning it. There is also no evidence for symmetric pairs of off-critical zeros, as would be required by the symmetry of the functional equations of zeta and the *L*-functions.

There are two additional ways we can compare ideas about the basis of the critical zeros. The first is the notion that the distribution of the zeta zeros reflects the statistics of random matrix theory. The zeros of zeta and their pair correlations have been shown to correspond to a GUE, or grand unitary ensemble. In fig 7b we thus compare these two statistics for the unreal zeros of *DL*(6,2) and the non-*L* function with quasi-character {0,1,0,0,-1,0} illustrated in fig 5 up to 2500*i*. Although it is true that *DL*(6,2), conforms a little more closely to the GUE statistic and there is more evidence for sustained phase-locking in the enhanced periodic fluctuations of the pair correlation, the idea that GUE is a defining indicator for criticality is less than convincing.

We can also examine the way in which convergent *DL* and non-*L* functions generate 'prime counting' functions using variants of the explicit formula above for zeta. We will use the simplified formula $\varphi(x) = \sum_{\substack{L(\rho)=0 \\ 0 \le \mathrm{Re}(\rho) < 1}} \frac{x^\rho}{\rho}$, $\rho = x + iy$ counting the zeros in the critical strip in order in

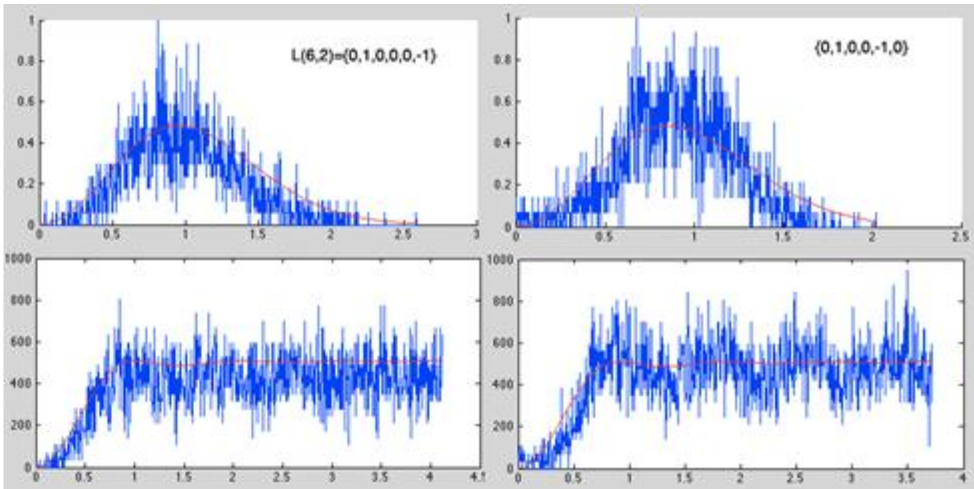

Fig 7b: (Above) distribution of the spacing of the zeros and (below) pair correlations for *DL*(6,2) with periodic zeros removed and the non *L* function with quasi-character {0,1,0,0,-1,0}. GUE distribution in red.

both directions from $y = 0$. In fig 7c the results are illustrated. Notably, both (5,2) and (6,2) correctly shift at primes and prime powers relatively prime to the period, but (6,2) does this only when the periodic zeros on x=0 are also included. Even more intriguing, the non –*L* function (0,1,0,0,-1,0} also counts shifts unperturbed by its off-critical zeros and correctly deletes shifts for terms having more than one factor in the series – i.e. 28=4x7, 52=4x13, 70-7x10,76=4x19 and 91=7x13.

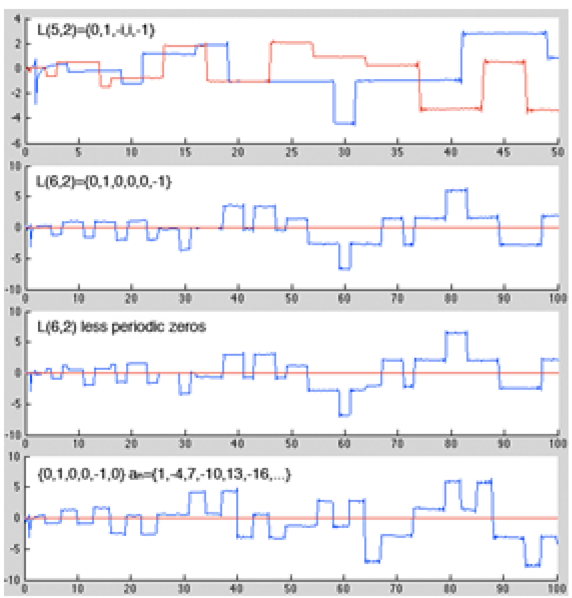

Fig 7c: *DL*(5,2) has a prime counting function with real and imaginary parts shifting precisely at primes $p\neq5$, and at powers of these primes according to $s(p^n)=\left(\chi(p)\right)^n$, χ={0,1,-*i*,*i*,-1}, reflecting the von Mangoldt definition above. There is no shift at integers with more than one prime factor. *DL*(6,2) has the same profile if the periodic zeros on x=0 are included, but if they are removed, spurious shifts occur at powers of 2. The non-*L* function (0,1,0,0,-1,0} forming an arithmetic progression a_n={1,-4,7,-10,13,-16,…} has shifts at each of the a_n except those which have more than one factor from the existing series.

We still lack a broad spectrum of examples lying outside zeta and the Dirichlet *L*-functions where the zeros are on the critical line or its displaced equivalent. Classically all the examples found comprise more general types of zeta and L-functions where the coefficients are determined by more arcane primal relationships, essentially guaranteeing the zeros are on-line through more veiled forms of primal non-phase-locking. In the following section we thus give a portrayal of the key types of abstract *L*-function, with a discussion of how their primal relationships arise.

Widening the Horizon to other types of Zeta and *L*-Function

To get a view of how *L*-functions can be extended beyond the context of Riemann and Dirichlet, a first stepping point is given by Dedekind zeta and Hecke *L*-functions of field extensions of the rationals $\boldsymbol{Q}$ (Garrett 2011). Here we look for the non-zero ideals of the ring of integers in a field extension. These also share features of analytic continuation using functional equations and Euler products. Some such as $Q[\sqrt{-5}]$ do not have unique prime factorizations and require consideration of the so-called class number, in this case 2, as $6 = 2.3 = (1+\sqrt{-5})(1-\sqrt{-5})$.

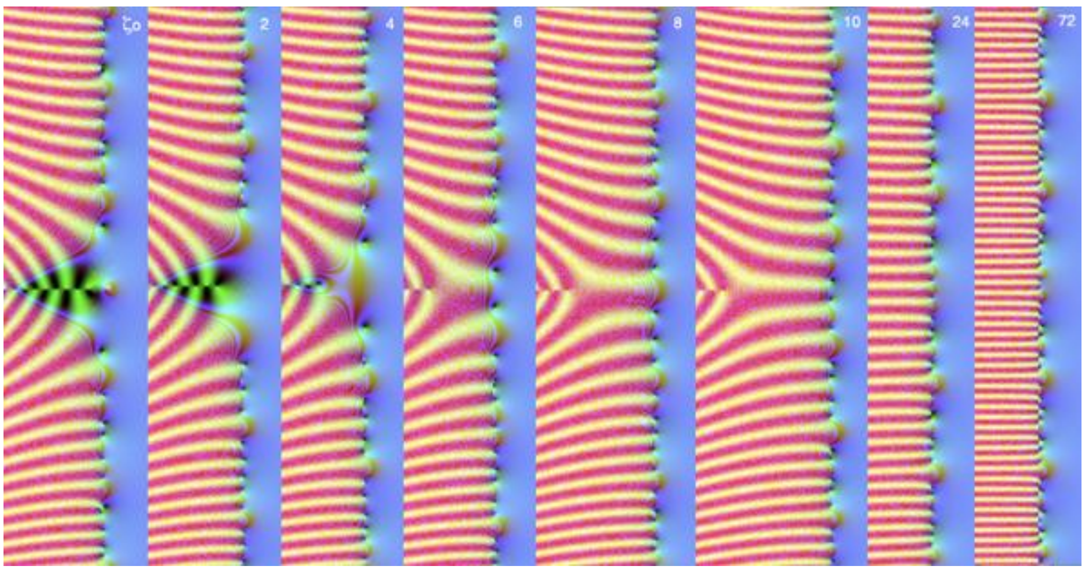

Fig 8: Profiles of the Dedekind zeta and Hecke *L*-functions for $\boldsymbol{Z}[i]$, the extension to the Gaussian integers. The portraits require both series representation, and the functional equation and Mellin transform theta integrals.

We will look at those of the Gaussian integers $\boldsymbol{Z}[i]$, defined by appending i to the integers, resulting in the lattice of complex numbers with integer real and imaginary parts. Here we have $N\alpha = \alpha\bar{\alpha} = |\alpha|^2$, so $\zeta_o = \sum_{0\neq\alpha\in o \bmod o^\times} \frac{1}{(N\alpha)^z} = \frac{1}{4}\sum_{m,n \text{ not both } 0} \frac{1}{(m^2+n^2)^z} = \prod_{\omega \text{ prime}} \frac{1}{1-(N\omega)^{-z}}$, where $N\alpha$ is the norm of the ideal $Z[i]/\alpha Z[i]$, which is uniquely expressible as an Euler product of prime ideals. This has a functional equation $\pi^{-z}\Gamma(z)\zeta_o(z) = \pi^{-(1-z)}\Gamma(1-z)\zeta_o(1-z)$, although, lacking an eta analogue, convergence isn't assured in the critical strip $0 < x < 1$, so Mellin transforms are commonly used to define the function more accurately there.

Correspondingly we have Hecke *L*-functions defined as follows. Consider the multiplicative group $\chi : Z[i] \to S^1$, $\chi(\alpha) \to (\alpha/\bar{\alpha})^l$, $l \in Z$. To give the same value on every generator this requires l to be trivial on units, hence $1=\chi(i)=\left(\frac{i}{-i}\right)^l=(-1)^l$, so $l\in 2Z$. We then have for each such l a Hecke L-function:

$$L(z,\chi)=\sum_{0\neq\alpha\in o \bmod o^\times}\frac{\chi(\alpha)}{(N\alpha)^z}=\frac{1}{4}\sum_{m,n\text{ not both }0}\frac{(\alpha/\bar{\alpha})^l}{(m^2+n^2)^z}=\prod_{\omega\text{ prime}}\frac{1}{1-\chi(\omega)(N\omega)^{-z}}$$ where the primes are now those of Gaussian integers, units ±1 or ±i times one of 3 types: 1+ i or a real prime which isn't a sum of squares (p mod 4 = 3), or has sum of real part squared and imaginary part squared a prime (p mod 4 = 1). Again we have a functional equation:

$$\pi^{-(z+|l|)}\Gamma(z+|l|)L(z,\chi)=(-1)^l\pi^{-(1-z+|l|)}\Gamma(1-z+|l|)L(1-z,\chi).$$

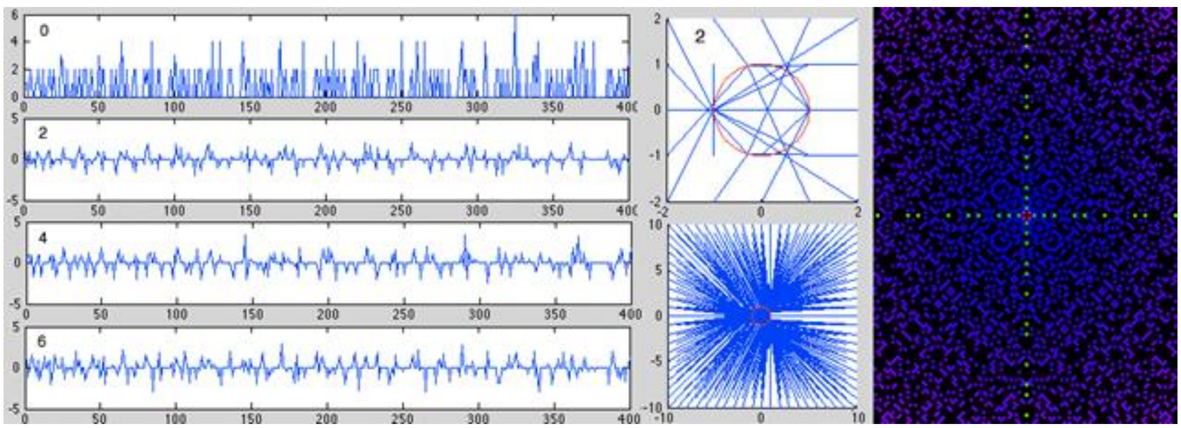

Fig 9: (Left) Profiles of the coefficients. Dedekind zeta (0) consists of the number of ways an integer can be represented as the sum of two integers divided by 4. The Hecke L-functions multiply these by the map $\chi:Z[i]\to S^1$, $\chi(\alpha)\to(\alpha/\bar{\alpha})^l$, $l\in 2Z$ to the unit circle illustrated (centre) for the case 2. Effectively this simply multiplies the angle of (m+in) by 2l and sets the modulus to 1 since $\chi(re^{i\theta})=(e^{i\theta}/e^{-i\theta})^l=e^{2li\theta}$, $l\in 2Z$. It therefore plays a role similar to the Dirichlet characters in evenly distributing the coefficients. All the coefficients are real and all but zeta fluctuate in sign. (Right) distribution of the Gaussian primes [r (±1±i), g (0,±4n+3) (±4n+3,0), b (m^2+n^2)= 4n+1: 4n+k prime]

The profiles of these functions with their analytic continuations are shown in fig 8, requiring, in addition to the functional equations, use of Mellin transform integral formulae in the critical strip:

$$\zeta_o(z)=\pi^z\Gamma(z)\int_1^\infty\left(y^z+y^{1-z}\right)\frac{\theta(iy)-1}{4y}dy,\ \theta(iy)=\sum_{m,n\in Z}e^{-\pi(m^2+n^2)y}=\left(\sum_{n\in Z}e^{-\pi n^2 y}\right)^2$$

$$L(z,\chi)==\pi^{z+|l|}\Gamma(z+|l|)\int_1^\infty\left(y^z+(-1)^l y^{1-z}\right)\frac{\theta_\chi(iy)}{4y}dy,\ \theta_\chi(iy)=\sum_{m,n\in Z}(m\pm in)^{2|l|}y^l e^{-\pi(m^2+n^2)y}$$

Counting the coefficients of the Dirichlet sum over the sums of squares, we find:

$$\zeta_0(z)=1+2^{-z}+0+4^{-z}+2\cdot 5^{-z}+0+0+8^{-z}+\ldots$$

In terms of our original primes in Z, we can say they fall into three cases, which will carry over to Hasse-Weil zeta functions: (i) **split** (p mod 4 = 1) two square roots of -1 in the finite (Galois) field F_{p^m} m>1 (see below); (ii) **inert** (p mod 4 = 3) no square root of -1 in F_{p^m}, m odd but 2 if m

even; (iii) **ramified** (p = 2) one square root of -1. Confirmation for 2, 3, 3^2, 5 and 7 is in appendix 2.
When we go back to Dedekind zeta's Euler product, we see that the product over Gaussian primes coincides exactly with an Euler product over integer primes incorporating the above cases and both generate the sum coefficients from unique prime power factorisations:

$$\prod_{\omega \text{ prime}} \frac{1}{1-(N\omega)^{-z}} = \left(\frac{1}{1-(1^2+1^2)^z}\right)\left(\frac{1}{1-(3^2)^z}\right)\left(\frac{1}{1-(1^2+2^2)^z}\right)\left(\frac{1}{1-(2^2+1^2)^z}\right)\ldots$$
$$= \frac{1}{1-(2)^z}\prod_{p \bmod 4=1}\frac{1}{(1-(p)^{-z})^2}\prod_{p \bmod 4=3}\frac{1}{1-(p)^{-2z}} = \left(\frac{1}{1-(2)^z}\right)\left(\frac{1}{1-(3)^{2z}}\right)\left(\frac{1}{(1-(5)^z)^2}\right)\ldots$$
$$= 1+2^{-z}+0+4^{-z}+2\cdot 5^{-z}+0+0+8^{-z}+\ldots$$

Alternatively, we can count the series terms directly in terms of a category mapping (functor) from commutative rings to sets, which preserves products and takes finite fields to finite sets (Baez). Effectively we are going to find how many ways make finite sets into semi-simple commutative rings, which are themselves always finite products of finite fields, which in turn have one field of q elements when $q=p^n$, p prime, and none otherwise, bringing in the powers of primes at a root level.

We can then make a general abstract Hasse-Weil zeta function $\zeta_s(z) = \sum_{n\geq 1}\frac{|Z_s(n)|}{n!}n^{-z}$ where $Z_s(n)$ are the species of different ways. To find the number of ways to make rings, we have to factor by the automorphisms of the finite fields that would make equivalent rings. The number of these turn out to be the number of automorphisms in each factor field times the number of permutations of equivalent factors. So we have for n = 0 , none; n =1, 1 (trivial ring an empty product of finite fields), n = 2, 1 (F_2); n = 3, 1 (F_3); n = 4, 2 (F_4 and F_2 x F_2); n = 5, 1; n = 6, 1 (F_2 x F_3); n = 7, 1,
n = 8, 3 (F_2 x F_2 x F_2, F_2 x F_4, F_8). Hence for all the cases up to 8 except 4 and 8 we have n!/1 ways, but for n = 4, we have 4!/2 + 4!/2 = 4! ways, the first from F_4 and the second from permutations of the F_2 factors. We find 8 similarly gives 8!/3 + 8!/2 + 8!/6 = 8! ways, so we find for the Riemann zeta function $\zeta(z) = \sum_{n\geq 1}\frac{n!}{n!}n^{-z} = \sum_{n\geq 1}n^{-z}$.
In the case of Dedekind zeta, each coefficient contains a number of ways combining the information from the number of roots of unity in each prime case with the above classification of the natural numbers, i.e. n = 0, 0; n = 1, 1x1!; n=2, 1x2!; n = 3, 0x3!; n = 4, 1x4!/2+1x4!/2=1x4!; n = 5, 2x5!; n = 6, (0x1)x6!; n = 7, 0x7!; n = 8, 1x8!/3 + 1x8!/2 + 1x8!/6 = 1x8! ways, leading again to: $\zeta_0(z) = 1+2^{-z}+0+4^{-z}+2\cdot 5^{-z}+0+0+8^{-z}+\ldots$.

This discussion leads on naturally to the next example of cubic curves where we see essentially the same picture of prime inertness, splitting or ramification, incorporated into an Euler product containing quadratic prime factors.

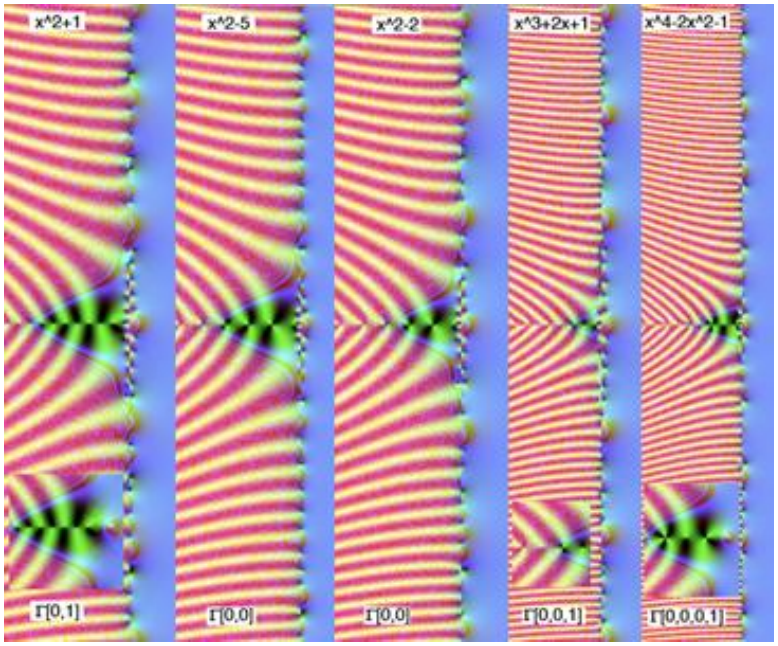

Fig 10: Dedekind zeta functions of a series of extension fields of polynomials portrayed with Dirichlet series and functional equation, but without the use of a Mellin transform in the critical strip, highlighting convergence failure of the Dirichlet series in the critical strip. Note the degenerate zeros in the left half plane caused by repeated gamma factors in the functional equation. Lower-right (inset) Computel Mellin transform portrait of the central valley, correcting the errors in the functional equation portrait.

L-functions of Elliptic Curves

The theory of elliptic curves and modular forms also generate *L*-functions (Booker 2008), which involve Euler products with quadratic factors in the denominator. In figs 11, 13 are illustrated a variety of abstract *L*-functions from the genus-1 *L*-function of the elliptic curve $y^2 + y = x^3 - 7x + 6$, through genus-2, 3 and 4 cases with repeated gamma factors causing multiple higher order zeros, to the *L*-function of a modular form based on the Ramanujan's Tau function , and many other cusp forms associated with elliptic curves. Simple scripts to list and generate L-functions of elliptic curves and diverse modular forms via Sage and PARI-GP using Tim Dokchitser's example files to generate the L-function coefficients and gamma factors for loading into RZViewer are included with the RZViewer package. Some simple Sage commands for elliptic curves and modular forms are illustrated in appendix 5.

Hasse-Weil *L*-functions of elliptic curves *E* are generated by taking the function $E(Q)$ over Q, or a field extension F, and estimating the number of rational points (Silverman 1986). Factoring mod p, for primes p, to get a set of A_p points on the curve $E(F_p)$ in the finite prime field F_p, given up to a maximum of $p+1$ points in F_p (including the point at infinity). We then let $a_p=p+1-A_p$ the number of missing points.

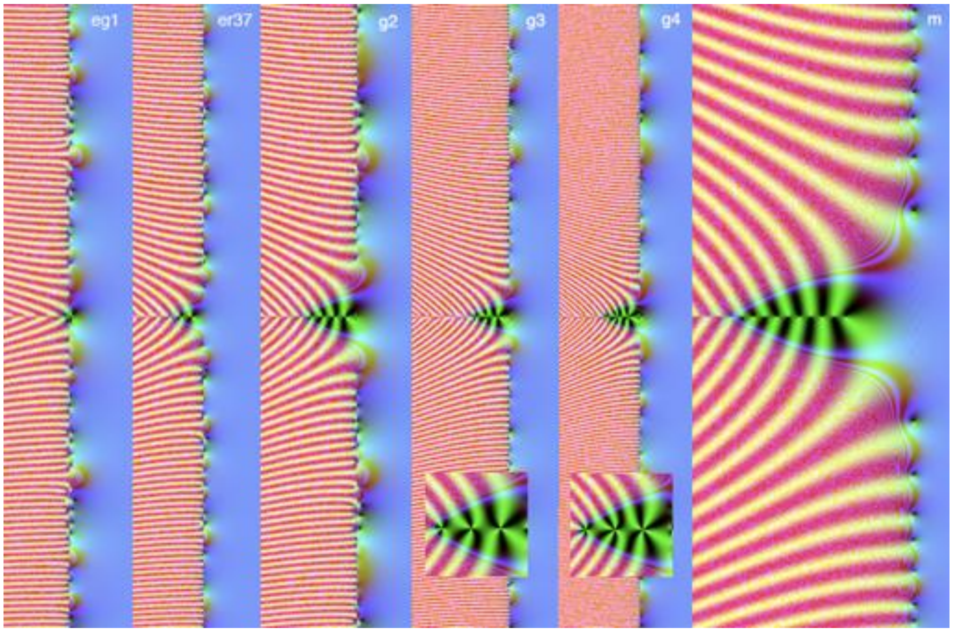

Fig 11: From left to right, L-functions of the genus-1 elliptic curve $y^2 + y = x^3 - 7x + 6$, the elliptic curve $y^2 + y = x^3 + 2x^2 + (19 + 8\omega)x + (28 + 11\omega),\ \omega = (1 + \sqrt{37})/2$ over $K = Q(\sqrt{37})$, the genus-2 curve $y^2 + (x^3 + x + 1)y = x^5 + x^4$, the genus-3 curve $y^2 + (x^3 + x^2 + x + 1)y = x^7 + 2x^6 + 2x^5 + x^4$, the genus-4 curve $y^2 + (x^5 + x + 1)y = x^7 - x^6 + x^4$, and the modular cusp form $\Delta(z) = \sum_{n \geq 1} \tau(n) e^{2\pi i n z}$, of weight 12, the modular discriminant, using Ramanujan's Tau function $\tau(n) = (5\sigma(n,3) + 7\sigma(n,5))\frac{n}{12} - 35\sum_{k=1}^{n-1}(6k - 4(n-k))\sigma(k,3)\sigma(n-k,5)$, where $\sigma(n,k) = \sum_{d \backslash n} d^k$. This is identical to the unique cusp form of weight ≤ 12 over $SL(2,Z) = \Gamma_1(1)$, mg1p1w12 in the notation of fig 15, and so occupies a place among modular cusp forms akin to that of the Riemann zeta function among Dirichlet L-functions.

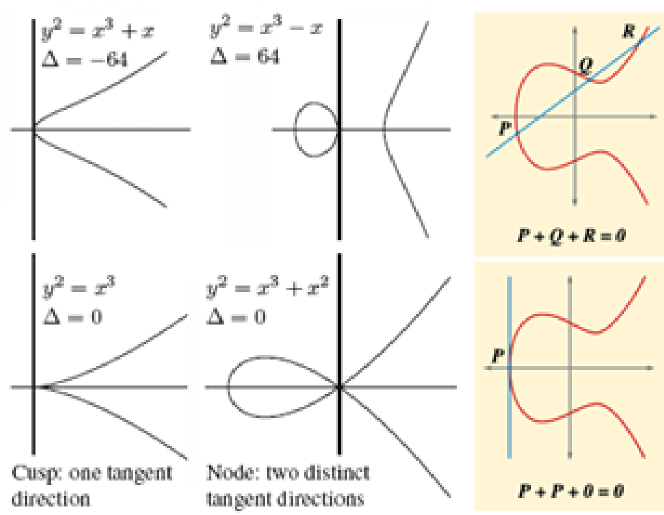

Fig 12: (Left) Examples of elliptic curves, (right) Group operation.

For example, for the elliptic curve $y^2 + y = x^3 - 7x + 6$, (0,2), (1,0), (1,4), (2,0), (2,4), (3,1), (3,3), (4,1), (4,3), (∞,∞) are solutions mod 5, giving a_5 = 5+1-10 = -4.

Hence we can define:

$$L(E,z) = \sum_{n=1}^{\infty} a_n n^{-z} = \prod L_p(E,z),\ L_p(E,z) = \begin{cases} \left(1 - a_p p^{-z} + p^{1-2z}\right)^{-1} & \text{good reduction} \\ \left(1 - a_p p^{-z}\right)^{-1} & \text{bad reduction} \end{cases}$$

where bad reduction i.e. a singularity of $E(F_p)$ results from repeated roots in $F_{p.}$, when $a_p = \pm 1$, depending on the splitting or inertness of p (rational or quadratic tangents of the node) for multiplicative reduction ($p|N$ but not p^2) of E, or is 0 if $p^2|N$ (additive reduction of the cusp), where N is the conductor, the 'effective' product of bad primes. Setting $L^*(E,z) = N^{z/2}(2\pi)^{-z}\Gamma(z)L(E,z)$, we have the functional equation $L^*(E,z) = \varepsilon L^*(E,2-z)$, where $\varepsilon = \pm 1$. The a_n are generated from the Euler product, convergent for x>3/2.

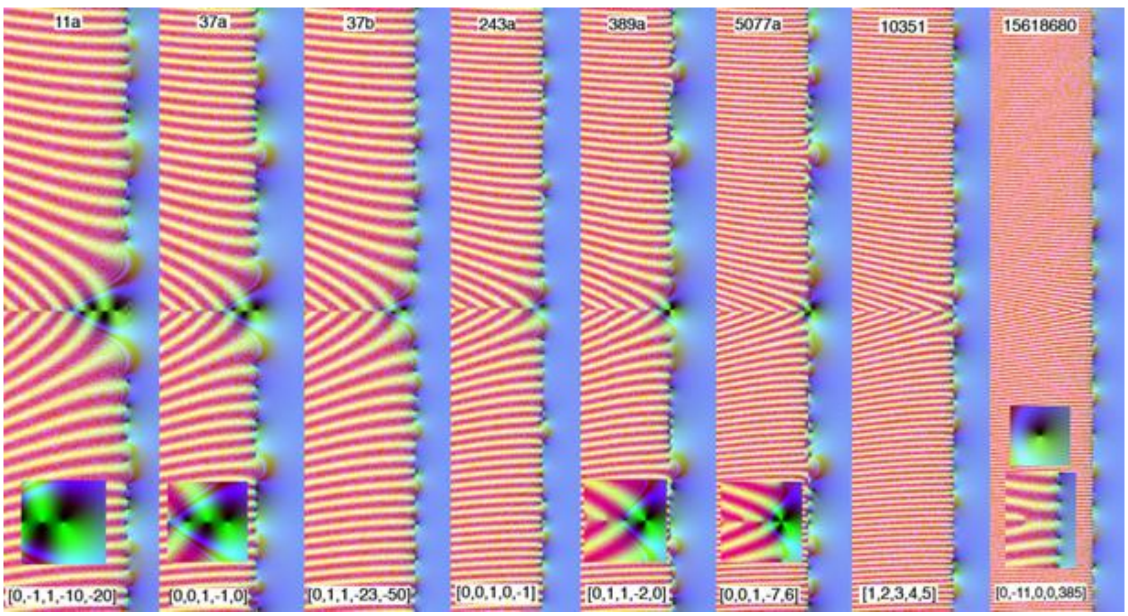

Fig 13: A menagerie of L-functions of elliptic curves over Q classified by their conductors (above) and their defining equations (below) where $[a,b,c,d,e]$ corresponds to $y^2 + axy + cy = x^3 + bx^2 + dx + e$. Inset Sage renditions of rank 0 (non-zero at 1), 1, 2 and 3 cases on $[-2,2]^2$ illustrating the Birch and Swinnerton-Dyer conjecture in the multiple-ray angular variation round the point. Unlike the higher-genus cases of fig 11, where repeated gamma factors cause multiple higher order zeros here it applies only to z = 1. See appendix 4 for computational method comparisons.

The conductor, as the 'effective' product, differs from the discriminant - a product of all bad prime factors. It consists of factors 1 for good reduction, p for multiplicative reduction, and p^2 for additive, except in the cases 2, 3 where the exponent may have an additional 'wild' component, increasing it up to 5 for 2 and 3 for 3, depending on the number of irreducible components (without multiplicity) of the 'special Neron fibre' (Tate, Silverman 1994).

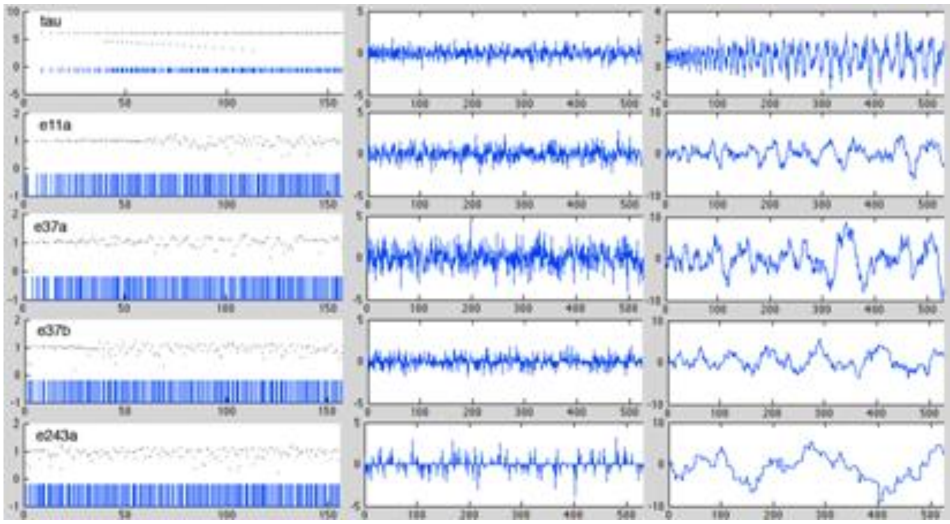

Fig 14: (Left): Newton's method on the Dirichlet series representation at 1000 terms for the modular form Delta and four elliptic curves of lowest conductor, in fig 13, show convergence to the critical line, for smaller imaginary values, similar to that of fig 6 for the Dirichlet *L*-function *L*(61,2), with convergence diminishing, as the conductor becomes larger, due to longer fluctuations in the sign of the coefficients, illustrated in the rescaled coefficients (centre) and additive trends (right). Tim Dokchitser's Computel, now in Sage, can give a more accurate numerical calculation for individual zeros using Mellin transforms, however these work only for limited imaginary values (<±30 for 37a) so there is no obvious way to accurately test the generalized RH for these *L*-functions. Moreover the Mellin transform method depends on established functional equations and we are interested in Dirichlet series because they are possessed by both *L*- and non-*L*-functions, which may not have a functional equation.

A good example is the elliptic curve $y^2 = x^3 - 11x^2 + 385$ (Lozano-Robledo), with additive reduction on 2, 11, split multiplicative on 5 and inert multiplicative on 7 and 461:

$$L(z) = \left(1-5^{-z}\right)^{-1}\left(1+7^{-z}\right)^{-1}\left(1+461^{-z}\right)^{-1}\prod_{p\neq 2,5,7,11,461}\left(1-a_p p^{-z}+p^{1-2z}\right)^{-1} = 1-\frac{2}{3^z}+\frac{1}{5^z}-\frac{1}{7^z}+\ldots\ ,$$

with conductor $N = 2^3\cdot 11^2\cdot 5\cdot 7\cdot 461 = 15618680$ and root number -1 (see fig 13).

Elliptic curves have a group multiplication connecting any two points on the curve to the third point of intersection of the line through them, as illustrated in fig 12. The Birch and Swinnerton-Dyer conjecture asserts that the rank of the abelian group $E(F)$ of points of E is the order of the zero of $L(E, z)$ at $z = 1$. Even rank gives ε=1 and odd ε=-1. The group may also have finite torsion elements.

Although the function depends on a rather arcane definition, through an elliptic curve, and then a quadratic Euler product, the resulting Dirichlet series is a standard sequence of coefficients, which possesses a standard functional equation and can thus be portrayed as a meromorphic function in C (analytic except for a finite number of simple infinities). For the elliptic curve $y^2 + y = x^3 - 7x + 6$, the first coefficients are: {1,-2,-3,2,-4,6,-4,0,6,8,-6,-6,-4,8,12,-4,-4,-12,-7,-8, …}.

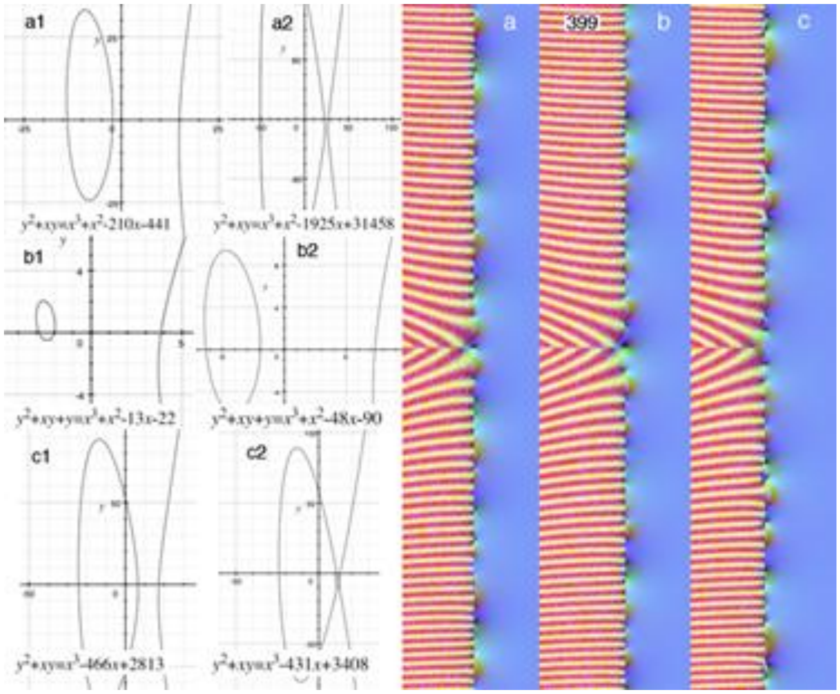

Fig 14b: *L*-functions of the elliptic curve conductor 399=3x7x19 come in three forms each of which has two elliptic curves associated with it. The space of modular cusp forms of weight 2 on gamma0 with conductor 399 has a dimension 53 and all three elliptic curve *L*-functions are linear combinations of several modular forrn basis functions (see fig 15).

If one takes the defining equation of an elliptic curve, one can generate an algebraic function, which is single-valued on a surface, enabling the elliptic curve to also be represented as a mapping of this surface. This parametrization, via the Weierstrass function and its derivative, defines a "fundamental parallelogram" in the complex plane, representing the two periodicities in the torus. The doubly periodic nature of the function and a one and three-holed torus (see modular forms) are illustrated below left, with the two periodicities illustrated on the one torus.

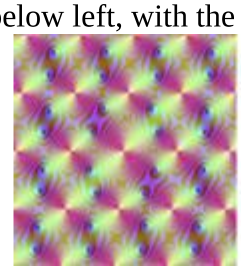


$$\wp(z;\omega_1,\omega_2)=\frac{1}{z^2}+\sum_{(m,n)\neq(0,0)}\left(\frac{1}{(z+m\omega_1+n\omega_2)^2}-\frac{1}{(m\omega_1+n\omega_2)^2}\right)$$

$$[\wp'(z)]^2=4[\wp(z)]^3-g_2\wp(z)-g_3,$$

$$g_2=60\sum_{(m,n)\neq(0,0)}(m\omega_1+n\omega_2)^{-4},\ g_3=140\sum_{(m,n)\neq(0,0)}(m\omega_1+n\omega_2)^{-6}$$

Elliptic functions over C are thus genus-1 curves, topologically equivalent to embeddings of a torus in PC x PC where PC is the complex projective plane or Riemann sphere derived by adding a single point at ∞ to C. Higher degree curves generate higher genus examples, as illustrated in fig 11.

Modular and Automorphic Forms

Complementing the L-functions of elliptic curves are those of modular forms. The toroidal nature of the elliptic function, causes it to be periodic on a parallelogram in C, resulting in a deep relationship with another kind of L-function. A modular function is a meromorphic function (analytic with poles) in the upper half-plane H, which is conserved by the modular group $SL(2,Z)$ of integer 2x2 matrices of determinant 1 i.e. $f(az+b)/(cz+d)=f(z)$. More generally we have modular of weight w (necessarily even) if $f(az+b)/(cz+d)= (cz+d)^w f(z)$. If it is holomorphic (fully analytic) in the upper half-plane (and at ∞) we say it is a *modular form*. If it is zero at ∞ we say it is a cusp form.

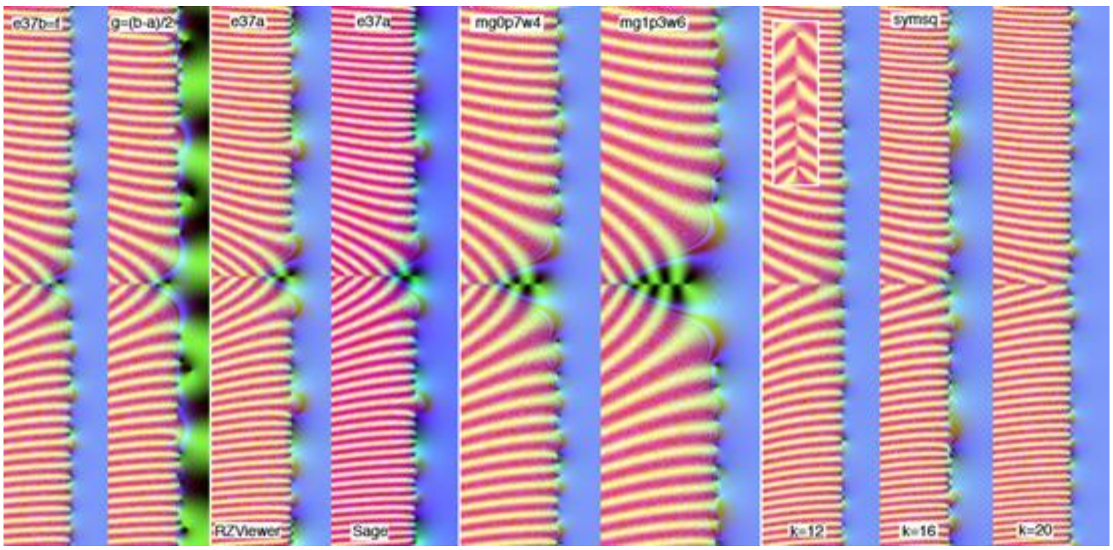

Fig 15: (Left): Functions f, g representing the 2 dimensions of modular cusp forms in $S_2(\Gamma_0(37)$. Here 37b has rank 0 with $\varepsilon = 1$, but 37a rank 1 with ε= -1. Consequently g has a complicated functional equation represented by $(b-a)/2$ for $x\geq 0$ and by $(b+a)/2$ for $x<0$. It also appears to have zeros manifestly off-critical. (Centre-left): Correspondence (see appendix 4) between portrait of e37a using RZViewer and an equivalent portrait using Computel Mellin transform algorithm via Sage. The left hand image takes 8 seconds and the right 4 hours on a Mac intel dual core at 2.1 GHz. (Centre-right) Two modular cusp forms mg0p7w4 and mg1p3w8 of gamma 0, 1, modulo 7, 3 and of weight 4, 6 respectively. In the latter case, and that of mg0p1w12 in fig 11, the gamma0 and gamma1 cusp forms are identical, but in general the gamma1 space has a higher dimension. For example there is only one elliptic L-function of conductor 5077 (see fig 13), but the gamm0 space has dimension 423 and the gamma 1 space dimension 1076535. If the weight is increased from 2 to 12 the dimension is even higher 11816505! (Right) Symmetric Square L-Functions of modular forms over $SL(2,Z)$ of weight k = 12, 16, 20 (Dummigan), having weight $4k$-3, with five Langlands gamma parameters [0, 1, 1-k, 2-k, 2-2k]. (Inset) k=12 negative real zeros showing varying degrees of degeneracy (rotated).

Since $f(z+1)=f(z)$, f is periodic, we can express it we can express it as a Fourier series in z or a Laurent series in q $f(z)=\sum_{n=-\infty}^{\infty} a_n e^{2\pi inz} = \sum_{n=-\infty}^{\infty} a_n q^n$. If f is meromorphic and has only simple poles we have only a finite number of negative powers of q and if f is holomorphic, we have a Taylor expansion $f(z)=\sum_{n=0}^{\infty} a_n e^{2\pi inz} = \sum_{n=0}^{\infty} a_n q^n$, $q = e^{2\pi inz}$. Using the Mellin transform

$M(f,z) = \int_0^\infty f(t)t^{z-1}dt$, we can derive the L-function $L(f,z) = (2\pi)^2 M(f,z)/\Gamma(z) = \sum_{n=1}^\infty a_n n^{-z}$, which again has a functional equation. If
$L^*(f,z) = N^{z/2}(2\pi)^{-z}\Gamma(z)L(f,z)$, then $L^*(f,z) = (-1)^{w/2} L^*(f,w-z)$, and L^* is meromorphic on C.

In the case of weight $w = 2$ there is thus a correspondence between the functional equations of elliptic curves and modular forms. The Taniyama-Shimura modularity theorem asserts that every elliptic curve over Q has a modular form parametrization based on the conductor, essentially through the periodicities induced by its toroidal embedding, a relationship pivotal in the proof of Fermat's last theorem (Daney), where Andrew Wiles (1995) showed that any semi-stable elliptic curve (having only multiplicative bad reductions) is modular. But if we can find $x^n + y^n = z^n$ then the elliptic curve $Y^2 = X(X - x^n)(X + y^n)$ is semi-stable but not modular. Hence the proof!

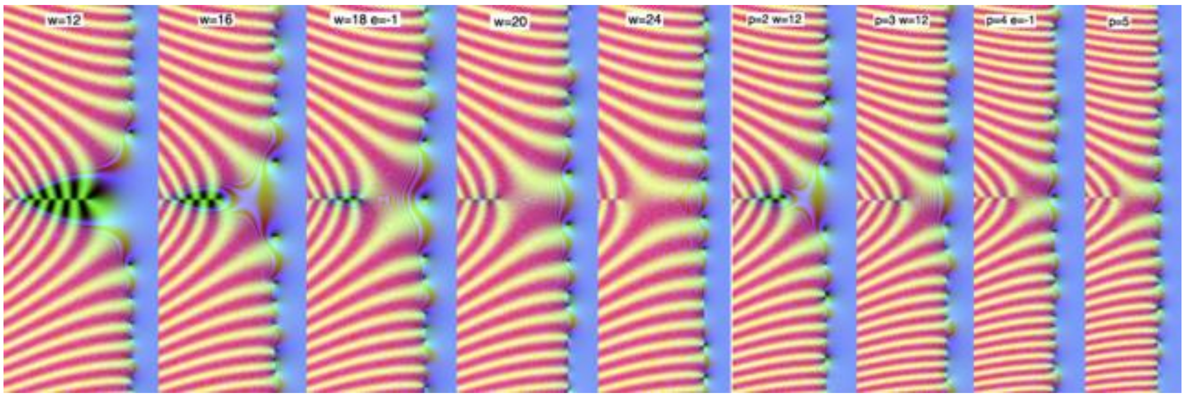

Fig 15a: (Left) Evolution of the principal Modular forms over $SL(2,Z)$ with increasing weight. (Right) Forms over $\Gamma_0(N)$ for increasing levels N with weight 12 have a similar evolution, with increasing dimensions of old and new forms.

We can find the modular form corresponding to a given elliptic curve as follows (Lozano-Robledo). Consider the modular group and congruence subgroups:

$$\begin{aligned}
\mathrm{SL}(2,\mathbb{Z}) &= \left\{\begin{pmatrix} a & b \\ c & d \end{pmatrix} : a,b,c,d \in \mathbb{Z},\ ad - bc = 1\right\}, \\
\Gamma_0(N) &= \left\{\begin{pmatrix} a & b \\ c & d \end{pmatrix} \in \mathrm{SL}(2,\mathbb{Z}) : c \equiv 0 \bmod N\right\}, \\
\Gamma_1(N) &= \left\{\begin{pmatrix} a & b \\ c & d \end{pmatrix} \in \Gamma_0(N) : a \equiv d \equiv 1 \bmod N\right\},
\end{aligned}$$

We now consider modular forms over congruence subgroups of $SL(2,Z)$ as above. Note that $\Gamma(N) \subset \Gamma_1(N) \subset \Gamma_0(N) \subset SL(2,Z)$, (where $\Gamma(N)$ also has $b \equiv 0$), so that a form in $\Gamma_0(N)$ is also in $\Gamma_1(N)$. For any congruence subgroup Γ_j there exists N so that $\Gamma_j(N) \subset \Gamma_j$ putting the form in $\Gamma_j(N)$. Since $M \setminus N \Rightarrow \Gamma_j(N) \subset \Gamma_j(M)$ a form in $\Gamma_j(M)$ is also in $\Gamma_j(N)$.

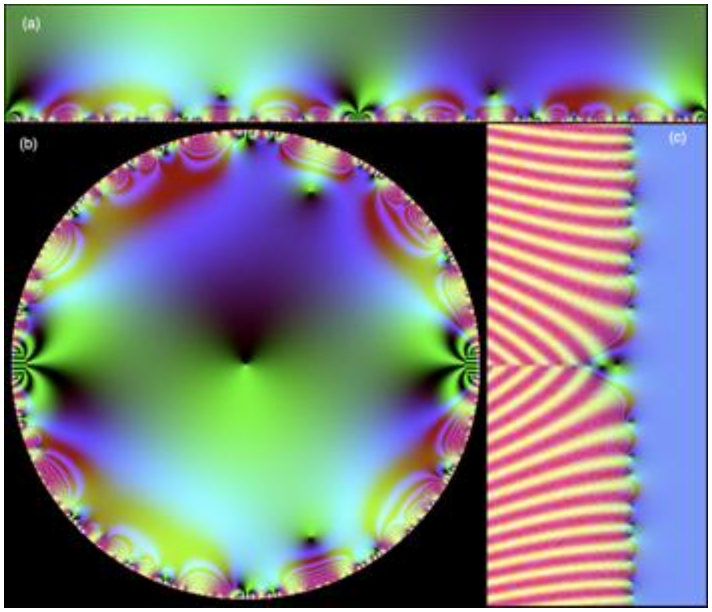

Fig 15b: (a) Modular cusp form over $S_2(\Gamma_0(26))$ represented as a Fourier series in the upper half-plane (a), as a function of q in the unit disc (b) and as a Dirichlet series L-function with a functional equation in the complex plane (c).

Setting $M_k(\Gamma_j(N))$ for the vector space of weight k modular forms and $S_k(\Gamma_j(N))$ for the subspace of cusp forms, we find that $M_2(\Gamma_0(11))$ is two dimensional and $S_2(\Gamma_0(11))$ is one-dimensional, generated by the function f with Taylor series in q having coefficients a_n={1, -2, 1, 2, 1, 2, 2, …} coinciding with those of $e11a$. The corresponding situation for $S_2(\Gamma_0(37))$ is a little more complicated, with M being three-dimensional generated by: $f(q) =q+q^3-2q^4-q^7-2q^9 +\ldots$, $g(q) =q^2+2q^3-2q^4+q^5-3q^6 +\ldots$ and $h(q)=1+2q/3+2q^2+8q^3/3+\ldots$, and S being two-dimensional, generated by f, g with corresponding attached L-functions as shown in fig 15. The dimension corresponds to the genus of a multi-hole torus embedding (Stein 2008). Turning to $e37a$, and $e37b$ with coefficients a={1, -2, -3, 2, -2, 6, -1, 0, 6, …} and b={1, 0, 1, -2, 0, 0, -1, 0, -1, …}, we find that $b = f$ and $a = f - 2g$, confirmed by the Taniyama-Shimura theorem, noting that linear combinations of modular forms are modular. Notice that $37b$ has rank 0 with $\varepsilon = 1$ while $37a$ has rank 1, with $\varepsilon = -1$. $S_2(\Gamma_0(N))$ is the direct sum of two subspaces S^+ and S^- because the linear operator w_N on $S_k(\Gamma_0(N))$ $w_N(f)(z) = i^k N^{-k/2} z^{-k} f(-(Nz)^{-1})$ is self-dual and thus has eigenvalues ±1. The w_n eigenfunctions possess the same type of functional equation as elliptic curve L-functions. In this case we have an eigenform basis a and b, however in the q^n echelon basis generated by Sage, g lies in neither subspace and has a composite functional equation (fig 15).

When we have a non-prime level N, there are both new forms and a spectrum of old forms arising from each of the factors of N. For each factor M, and $d|(N/M)$ we have the modular function $f(q^d)$ as well as $f(q)$ of level M. For example in the case of N=38, there are two old forms, which in terms of the Hecke operators, (see below) are eigenforms. These are the elliptic curve L-function $e19$ and the related L-function $2^{-z}L(e19)$, viz: $L_{e19}(z) = 1^{-z} + 0\cdot 2^{-z} - 2\cdot 3^{-z} + \ldots$, with $g(q) = q - 2q^3 + \ldots$. We also have $g(q^2) = q^2 - 2q^6 + \ldots$, with L-function $L_{e19x2}(z) = 2^{-z} + 0\cdot 4^{-z} - 2\cdot 6^{-z} + \ldots = 2^{-z} L_{e19}(z)$.

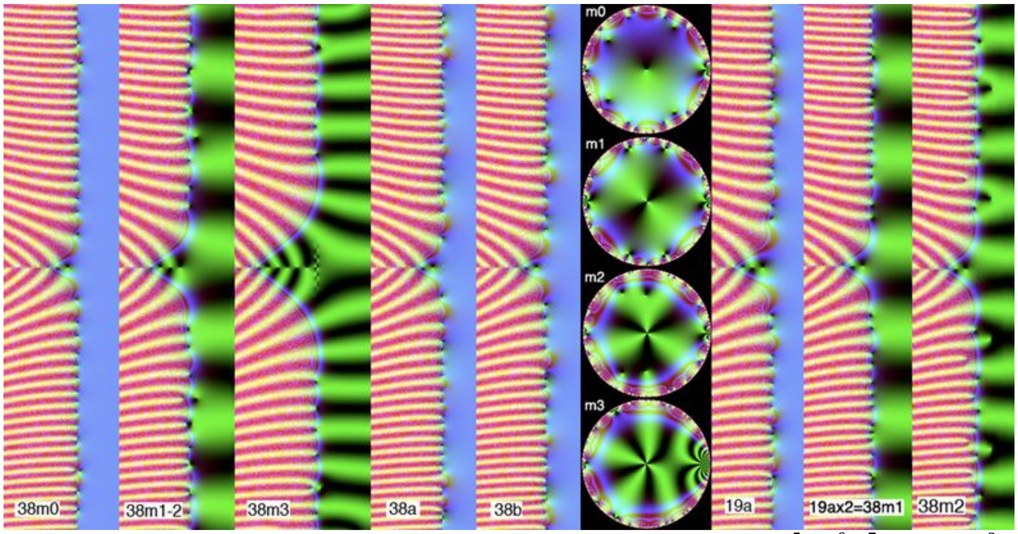

Fig 15c: (Left) $S_2(\Gamma_0(38))$ has basis vectors m_0-m_3, in echelon-form in q^n, e.g. $m_0=q-q^5-2q^6-q^7+\ldots$, $m_1=q^2-2q^6-2q^8+\ldots$, $m_2=q^3+q^5-2q^6+\ldots$, $m_3=q^4-3q^5+q^6+\ldots$, with the elliptic curves being combinations $a=m_0-(m_1-m_2)+m_3$ and $b=m_0+(m_1-m_2)+m_3$. In this case both elliptic curves have $\varepsilon = +1$. (Centre) the power series of m_0-m_3 in terms of q in the unit disc. (Right) There are also two old eigenforms comprising $e19$ and $2^{-z}L(e19)=m_1$. The linear combination $m19=e19=m_0-2m_2-2m_3$, illustrates the fact that the space of modular forms of level N includes those of M: $M|N$. We also have $e19\text{x}2=m_1$ giving 4 eigenforms, so can perform a functional equation reconstruction of the four m_i by inverting the matrix defining the elliptic curve eigenforms in terms of the q^n echelon basis. Although each of the m functions shown left also have functional equations with $\varepsilon = +1$, m_2 lies in neither S^+ nor S^-, for N=19 or 38, as with g of $S_2(\Gamma_0(37))$. Again the m_i , being superpositions of eigenforms appear to have off-critical zeros, while the eigenforms a, b, $e19$ and $e19$x2 do not.

At another extreme, the space of modular forms over $SL(2,Z)$ of weight 12 has 2 dimensions, with basis vectors represented by the form Δ of the τ function illustrated in fig 11 and the normalized Eisenstein series E_{12} where $E_{2k} = 1 + \dfrac{2}{\zeta(1-2k)}\sum_{n=1}^{\infty}\sigma(n,2k-1)q^n$, each of which is a modular form of weight *2k over* $SL(2,Z)$. Eisenstein series are defined by $G_{2k}(z) = \sum_{m,n \in Z^2 \setminus (0,0)} (m+nz)^{-1}$ with $q = e^{2\pi i n z}$ as above, with further generalizations to $m,n \equiv 0 \bmod N$ for $\Gamma_j(N)$. This doesn't have an L-function because the 1 makes it not a cusp form, but the coefficients generated by the divisor function do coincide with the sigma function $\zeta(z)\zeta\big(z-(2k-1)\big)$ of fig 21, thus giving an illustration of the two eigenforms. In many ways the modular forms of weight 2 are atypical as Eisenstein series only begin with weight 4.

The symmetric square lift (see fig 15) is defined as follows. Given a form f over $SL(2,Z)$ with Euler product, $L(z,f) = \prod_{p \text{ prime}} \left(1 - a_p p^{-z} + p^{-2z}\right)^{-1} = \prod_{p \text{ prime}} \left(1 - \alpha_f(p)p^{-z}\right)^{-1}\left(1 - \alpha_f(p)^{-1}p^{-z}\right)^{-1}$ where $a_p = \alpha_f(p) + \alpha_f(p)^{-1}$, the symmetric square lift is a $GL(3)$ form ϕ with Euler product

$$L(z,\phi)=\prod_{p\text{ prime}}\left(1-A(1,p)p^{-z}+\overline{A(p,1)}p^{-2z}-p^{-3z}\right)^{-1}=\prod_{p\text{ prime}}\left(1-\alpha_\phi(p)p^{-z}\right)^{-1}\left(1-\beta_\phi(p)p^{-z}\right)^{-1}\left(1-\gamma_\phi(p)p^{-z}\right)^{-1}$$

where $\begin{pmatrix}\alpha_\phi(p) & & \\ & \beta_\phi(p) & \\ & & \gamma_\phi(p)\end{pmatrix}=\begin{pmatrix}\alpha_f(p)^2 & & \\ & 1 & \\ & & \alpha_f(p)^{-2}\end{pmatrix}$ (Dummigan, Bian).

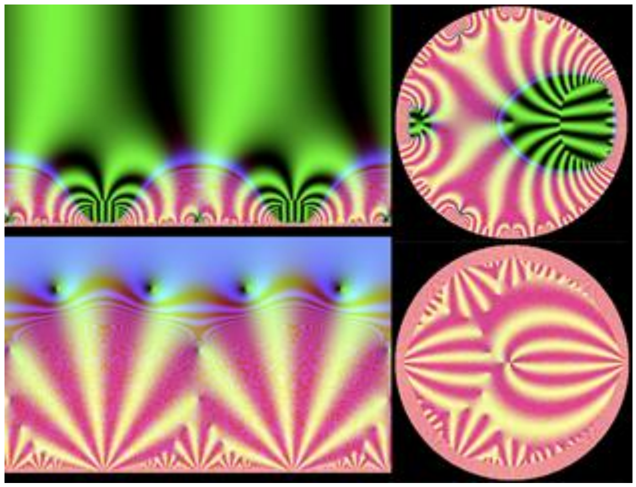

Fig 15d: Fourier and Taylor representations of the Tau and Eisenstein functions of weight 12 in addition to the *L*-function portraits of figs 11 and 21.

Each of the types of *L*-function discussed admit a functional equation determined by the Dirichlet series, a finite number of gamma (Hodge, or Langlands) parameters, determined by the underlying topology generating the Euler product, the conductor, and a sign factor (Dokchitser, Harron):

$$L^*(f,z)=N^{z/2}(2\pi)^{-z}\Gamma\left(\frac{z+\lambda_1}{2}\right)\ldots\Gamma\left(\frac{z+\lambda_d}{2}\right)L(f,z),\text{ then }L^*(f,z)=\varepsilon L^*(f,w-z)$$

where $|\varepsilon|=1,\ \varepsilon=e^{2\pi ik/n}$ for Dirichlet *L*-functions $\varepsilon=\pm1$ otherwise. The gamma factors can be used to define a generalized Mellin transform technique for describing *L*-functions in the critical strip for moderate *y* values (Dokchitser). These types can be generalized in motivic *L*-functions (Deligne, Dokchitser). The Langlands program (1980) of automorphic forms includes a comparable explanation of Euler products involving polynomials of higher degree.

Modular forms that are eigenfunctions of all Hecke operators $T_nf=\lambda_nf=a_nf$, where $T_nf(z)=n^{k-1}\sum_{M\in\Gamma\backslash M_n}(cz+d)^{-k}f\left(\frac{az+b}{cz+d}\right),\ M_n=\left\{A=\begin{pmatrix}a&b\\c&d\end{pmatrix}:|A|=n\right\}$, have the equivalent Euler product $L(f,z)=\prod_{p|N}(1-a_pp^{-z})^{-1}\prod_{p\nmid N}(1-a_pp^{-z}+p^{2k-1-2z})^{-1}$ (Cogdell, Lozano-Robledo).

Conveniently each eigenfunction satisfies all the Hecke operators T_n simultaneously.

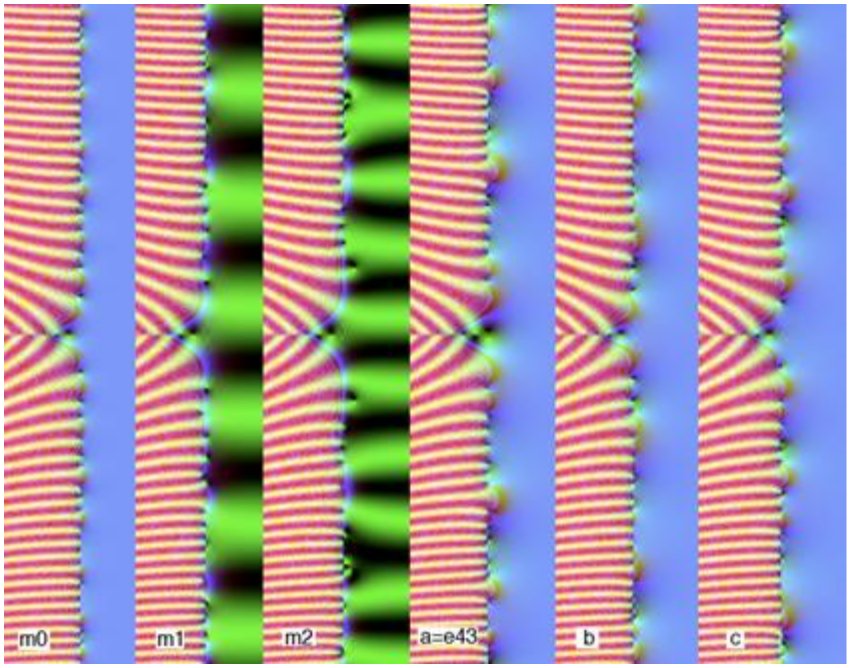

Fig 15e: The situation for level N=43 presents new features. The cusp space has three dimensions and there are also three eigenfunction newforms *a*, *b*, *c*, the first of which is identical to elliptic *e*43, which has root -1. The two additional root 1 eigenforms have Hecke eigenvalues $\pm\sqrt{2}$, and do not correspond to elliptic curves. Hence there are sufficient eignfunctions to represent the *q*-echelon basis forms in terms of the combined eigenfunction equations (left).

One can calculate Hecke operators and matrices in terms of the power series $f(q) = \sum_m a_m q^m$ as follows:

$T_p(f(q)) = \sum_{m \in Z} (b_m q^m = \sum_{m \in Z} (a_{mp} + p^{k-1} a_{m/p}) q^m$, $a_{m/p} = 0,\ m/p \notin Z$, p prime, which is generally sufficient for determining eigenvalues and eigenforms.

For example for N=43, we have echelon basis: $f = q + 2*q^5 - 2*q^6 - 2*q^7 - q^9 + O(q^{10})$, $g = q^2 - 1/2*q^4 + q^5 - 3/2*q^6 - q^8 - 1/2*q^9 + O(q^{10})$, $h = q^3 - 1/2*q^4 + 2*q^5 - 3/2*q^6 - q^7 + q^8 - 1/2*q^9 + O(q^{10})$ Applying the above formula for T_2 to f, we have $b_1 = a_2 + 2.0 = 0$, $b_2 = a_4 + 2.0 = 2$, $b_3 = a_6 + 2.0 = -2$, giving the first row of the Hecke matrix $T_2 = \begin{bmatrix} 0 & 2 & -2 \\ 1 & -1/2 & -3/2 \\ 0 & -1/2 & -3/2 \end{bmatrix}$, which has eigenvalues a_0 = -2 and $a_1 = \pm\sqrt{2}$. These eigenvalues give normalized eigenvectors $v = q - 2*q^2 - 2*q^3 + 2*q^4 - 4*q^5 + 4*q^6 + q^9 + O(q^{10})$, $w_{a1} = q + a_1*q^2 - a_1*q^3 + (2-a_1)*q^5 - 2*q^6 + (a_1 - 2)*q^7 - 2*a_1*q^8 - q^9 + O(q^{10})$, which are *newforms*, normalized eigenforms of level N not arising from an $M < N$, defined as a linear combination of the above echelon basis functions, the first of which is the elliptic curve *e*43*a*. One can confirm they are eigenvectors using the same formula, e.g.

$T_2(v) = -2v$. By inverting the resulting basis transformation matrix $A = \begin{bmatrix} 1 & -2 & -2 \\ 1 & \sqrt{2} & -\sqrt{2} \\ 1 & -\sqrt{2} & \sqrt{2} \end{bmatrix}$, we can in turn express the echelon basis in terms of the eigenforms. Each elliptic function with conductor N is thus associated with a *newform* - (Stein).

Computing the original echelon basis is more complicated (Stein). For forms over $SL(2,Z)$ such as those of weight 24 in fig 15a, we can derive a basis for the three dimensional modular space based on Eisenstein series namely: $E_4^{\,6}$, $E_4^{\,3}E_6^{\,2}$, $E_6^{\,4}$ and then perform row operations to gain a q^n echelon basis called the Miller basis, which has two dimensions of cusp forms. Computing the bases of cusp forms over $S_2(\Gamma_0(N))$ is complicated and most conveniently done using modular symbols, which are representations of homology classes of paths on the embedded multi-hole torus whose genus determines the dimension of the modular space, represented on the upper half plane between rational points on the real line (including the point at ∞). Modular symbols have relations such as $\{\alpha,\beta\}+\{\beta,\gamma\}+\{\gamma,\alpha\}=0,\ \{\alpha,\alpha\}=0,\ \{\alpha,\beta\}=-\{\beta,\alpha\}$ and are acted on by rational matrices $g\{\alpha,\beta\}=\{g(\alpha),g(\beta)\}$, can be readily computed using Sage by a technique derived by Manin using continued fractions, and are compatible with Hecke operators (Stein).

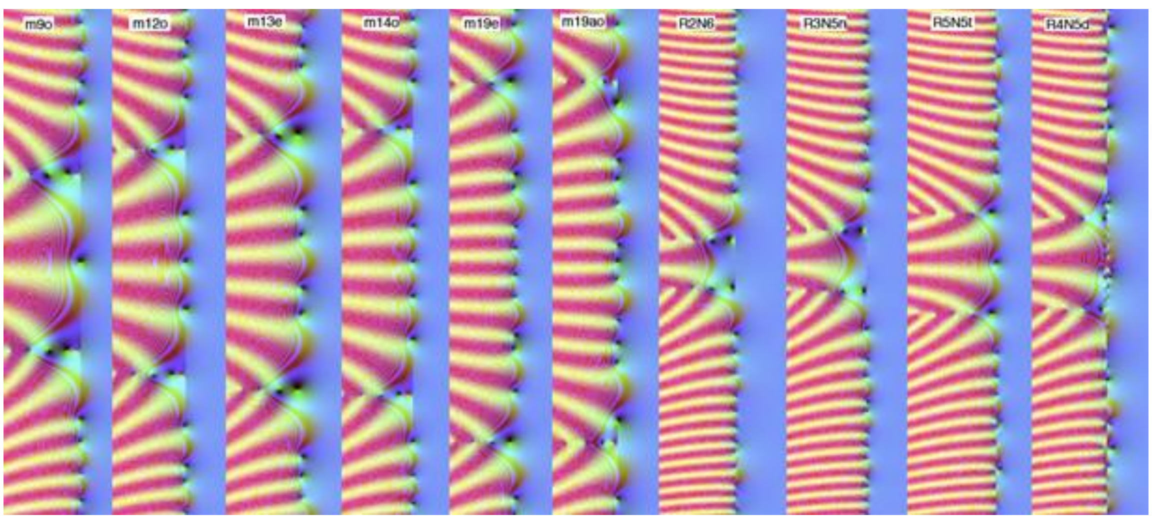

Fig 15f: L-functions of Maass forms over $PSL(2,Z)$ with eigenvalues 9.5336, 12.1730, 14.3585, 19.4847 (odd) and 13.7797, 19.4234 (even) and three forms over Γ_0 with N=6, 5, 5, 5 eigenvalues 2.5923, 3.2642, 5.4361, 4.8937, the last of which has a double eigenvalue with two conjugate L-functions.

Maass forms are modular differential functions satisfying the hyperbolic Laplace wave function $\Delta = -y^2\left(\frac{\partial^2}{\partial x^2}+\frac{\partial^2}{\partial y^2}\right)$, which commutes with $SL(2,Z)$, and generates a vast spectrum of eigenforms, having complex gamma factors $\lambda_i = e \pm ir,\ i=1,2$, where e=0,1 and $\varepsilon = 1,-1$ for even and odd functions respectively where the eigenvalue is $\frac{1}{4}+r^2$, and a slightly more complicated Fourier series $f(z)=\sqrt{y}\sum_{n=1}^{\infty} a_n K_{ir}(2\pi\,|\,n\,|\,y)e^{2\pi ix}$, with K_{ir} the modified Bessel function. For N=11 there are around 1000 such forms over Γ_0 (Booker et. al. 2006, Farmer and

Lemurell), which can be located by searching for eigenvalue hot spots. Several Maass form *L*-functions are illustrated in fig 15f.

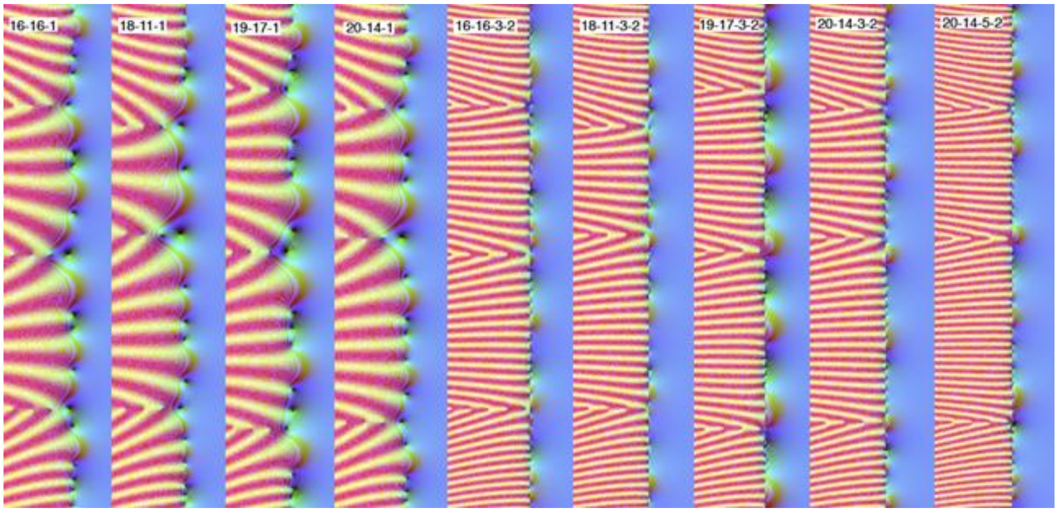

Fig 15g: Third degree transcendental Maass form *L*-functions. First views of the *L*-function profiles for the above parameters for three selections of Dirichlet character.

A new class of *L*-function (Bian 2010, Booker 2008) has been discovered, based on automorphic *GL*(3) Maass forms, which are written in terms of a three dimensional generalized upper half-plane *w*=*XY*, where $X=\begin{pmatrix}1 & x_2 & x_3\\ 0 & 1 & x_1\\ 0 & 0 & 1\end{pmatrix}$, $Y=\begin{pmatrix}y_1y_2 & 0 & 0\\ 0 & y_1 & 0\\ 0 & 0 & 1\end{pmatrix}$, $x_i, y_i \in R,\ y_i > 0$. The form $\varphi(w)$ is an eigenfunction of the Laplacian, which is preserved under *SL*(3,*Z*). This has an extended Fourier series, which can be used to define a complex *L*-function with a degree 3 Euler product

$$L(z,\varphi\times\chi)=\prod_{p\ \text{prime}}\left(1-A(1,p)\chi(p)p^{-z}+A(p,1)\chi^2(p)p^{-2z}-\chi^3(p)p^{-3z}\right)^{-1}$$

where $\chi(p)$ is a Dirichlet character 'twisting' the *L*-function and *A*(*p*,*q*) are Fourier coefficients of the Maass cusp form with eigenvalues (λ_1,λ_2), $\text{real}(\lambda_i)=1/3$.

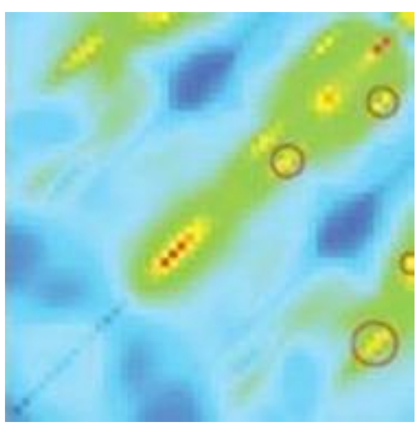

Fig 15h: Hot regions in (*u*,*v*) =[10, 20]2 (red) with 4 non-trivial degree 3 examples circled (18.902, 11.761), (16.741, 16.232), (20.021, 14.070), (19.179, 17.702) and quasi-trivial examples on the diagonal *u* = *v* at 13.779, 17.738, 19.423 (Bian)

In particular $A(1,p)=\overline{A(p,1)}$. Bian has found locations in parameter space $(u,v),\ \lambda_1=(1+ui)/3, \lambda_2=(1+vi)/3$ defined in terms of the gamma function imaginary parameters $\alpha=-(u+2v)i/3,\ \beta=(2u+v)i/3,\ \gamma=(-u+v)i/3$ where non-trivial transcendental degree 3 *L*-functions, not being simply a product of degree 1 or degree 1 and 2 Euler products, nor symmetric square lifts (fig 15) of a quadratic Euler function, occur. These also obey a functional equation of the form $\Lambda(z,\varphi\times\chi)=\varepsilon_\chi^3\Lambda(1-z,\tilde{\varphi}\times\bar{\chi})$, where ~ takes coefficients and gamma factors to their conjugates, and

$$\Lambda(z,\varphi\times\chi)=N^{z/2}\pi^{-(z-\alpha)/2}\Gamma\left(\frac{z-\alpha}{2}\right)\pi^{-(z-\beta)/2}\Gamma\left(\frac{z-\beta}{2}\right)\pi^{-(z-\gamma)/2}\Gamma\left(\frac{z-\gamma}{2}\right)L(z,\varphi\times\chi).$$

The upshot of this study of a reasonable spread of *L*-functions and non-*L* counterparts, is that the non-trivial zeros lie on the weighted critical line only if they are generated by an underlying non-mode-locked primal distribution, despite the fact that the Dirichlet sum is over all integers and the relationship with the Euler product over primes holds only outside the critical strip in the right half-plane. This suggests widening the approach to consider more general classes of Euler products.

References

Baez, John *Zeta functions* http://ncatlab.org/johnbaez/show/Zeta+functions
Balanzario E, Sanchez-Ortiz J (2007) *Zeros Of The Davenport-Heilbronn Counterexample* Mathematics Of Computation 76/260, 2045–2049.
Bian, Ce (2010) *Computing GL(3) automorphic forms* Bull. London Math. Soc. 42 (2010) 827–842. Ce Bian's website with code: http://www.maths.bris.ac.uk/~macxb/
Enrico Bombieri and Amit Ghosh (2011) *Around the Davenport-Heilbronn function* Russ. Math. Surv. 66 221 doi: 10.1070/RM2011v066n02ABEH004740 http://iopscience.iop.org/0036-0279/66/2/R02
Booker, A (2006) *Turing and the Riemann Hypothesis* Notices of the American Mathematical Society 53/10 1208-11.
http://www.ams.org/notices/200610/fea-booker.pdf
Booker, Andrew (2008) *Uncovering a New L-function* Notices of the American Mathematical Society 55/9 1088-94. http://www.staff.science.uu.nl/~plaza101/Booker.pdf
Booker A, Strombergsson A, Venkatesh A (2006) *Effective Computation of Maass Cusp Forms* IMRN International Mathematics Research Notices, Article ID 71281, 1-3. http://www2.math.uu.se/~astrombe/papers/bsv27april06.pdf
Computer code and coefficients: http://www2.math.uu.se/~astrombe/emaass/emaass.html
Peter Borwein, Greg Fee, Ron Ferguson, and Alexa van der Waall (2000) *Zeros of Partial Sums of the Riemann Zeta Function* Experimental Mathematics 16:1, 21
Bump D, Ginzburg D (1992) *Symmetric Square L-Functions on GL(r)* Annals of Mathematics 136 137-205. http://www.jstor.org/stable/2946548
Cloitre B. (2011) *A tauberian approach to RH* http://arxiv.org/abs/1107.0812
Cogdell J *Lectures on L-functions, Converse Theorems, and Functoriality for* GL_n http://www.prime.sdu.edu.cn/cimpaschool/fields.ps
Conrey, J. Brian (2003), *The Riemann Hypothesis* Notices of the American Mathematical Society 50/3 341-353, http://www.ams.org/notices/200303/fea-conrey-web.pdf.
Cremona J (2011) Elliptic Curve Data http://www.warwick.ac.uk/~masgaj/ftp/data/
Daney Charles The Mathematics of Fermat's Last Theorem http://cgd.best.vwh.net/home/flt/flt01.htm
Davenport, H., Heilbronn, H., (1936) *On the zeros of certain Dirichlet series I, II*. J. London Math.Soc. 11, 181-185, 307-312.
Deligne P (1979) *Valeurs de fontions L et périodes d'intégrales* Proceedings of the Symposium in Pure

Mathematics,
33.2, Providence, RI: AMS, pp. 313–346, http://www.ams.org/online_bks/pspum332/pspum332-ptIV-8.pdf
Dokchitser, Tim (2002) *Computing special values of motivic L-functions* http://arxiv.org/abs/math.NT/0207280 http://www.dpmms.cam.ac.uk/~td278/computel/ See also: http://www.sagemath.org/
Dummigan N (2001) *Symmetric Square L-Functions and Shafarevich–Tate Groups* Experimental Mathematics 10/3 384-400 http://www.neil-dummigan.staff.shef.ac.uk/papers.html
Farmer D, Lemurell S *Maass Form L-Functions*
http://www.math.chalmers.se/~sj/forskning/level11_2a.pdf
Franel, J.; Landau, E. (1924), *Les suites de Farey et le problème des nombres premiers*, Göttinger Nachr.: 198-206
Galois, Évariste (1846). "*OEuvres mathématiques d'Évariste Galois.*". Journal des mathématiques pures et appliquées
XI: 381–444. http://visualiseur.bnf.fr/ark:/12148/cb343487840/date1846.
Garrett, Paul (2011) *Analytic continuation, functional equation: examples*
http://www.math.umn.edu/~garrett/m/mfms/notes_c/analytic_continuations.pdf
Gun S, Ram Murty M, Rath P (2010) *Transcendental Nature of Special Values of L-Functions* Canadian Journal of Mathematics doi:10.4153/CJM-2010-078-9 http://www.mast.queensu.ca/~murty/cjm2.pdf
Harron R (2010) Critical integers of motivic L-functions and Hodge numbers
http://math.bu.edu/people/rharron/research/CriticalIntegers.pdf
Hughes J. Shallit J., (1983) *On the Number of Multiplicative Partitions*, American Mathematical Monthly, 90(7) 468–471.
Ingham, A.E. (1932, rep 1990), The Distribution of Prime Numbers, Cambridge University Press, MR1074573, ISBN 978-0-521-39789-6
Ivic A (2003) *On Some reasons for Doubting the Riemann Hypothesis* in Peter B. Borwein (ed.) The Riemann hypothesis: a resource for the afficionado and virtuoso alike, Springer.
King C.C. (2009-2011) Riemann Zeta Viewer http://www.dhushara.com/DarkHeart/RZV/RZViewer.htm
King C.C. (2009) Experimental Observations on the Uncomputability of the Riemann Hypothesis
http://www.dhushara.com/DarkHeart/RH2/RH.htm
King C.C. (2011) *Fractal Geography of the Riemann Zeta Function* http://arxiv.org/abs/1103.5274
http://www.dhushara.com/DarkHeart/geozeta/zetageo.htm
Knopfmacher A, Mays M (2006) *Ordered and Unordered Factorizations of Integers* The Mathematica Journal 10:1 ©
Wolfram Media, Inc. http://www.mathematica-journal.com/issue/v10i1/contents/Factorizations/Factorizations.pdf
Langlands, Robert P. (1980), *L-functions and automorphic representations*, Proceedings of the International Congress
of Mathematicians (Helsinki, 1978), 1, Helsinki: Academia Scientiarum Fennica, pp. 165–175,
http://mathunion.org/ICM/ICM1978.1/Main/icm1978.1.0165.0176.ocr.pdf
Lozano-Robledo, Álvaro (2009) *Elliptic Curves, Modular Forms and their L-functions* Student Mathematical Library
Ias/Park City Mathematical Subseries, Volume: 58
http://www.math.uic.edu/~wgarci4/pcmi/PCMI_Lectures.pdf
Odlyzko A. (1992) *The 10^20-th zero of the Riemann zeta function and 175 million of its neighbors*
http://www.dtc.umn.edu/~odlyzko/unpublished/index.html
Odlyzko, Andrew (2002) *Zeros of the Riemann zeta function: Conjectures and computations*
http://www.dtc.umn.edu/~odlyzko/talks/riemann-conjectures.pdf
Odlyzko, A., te Riele, H. (1985), *Disproof of the Mertens conjecture*, Journal für die reine und angewandte Mathematik 357: 138–160.
Riemann, Bernhard (1859), *Über die Anzahl der Primzahlen unter einer gegebenen Grösse*, Monatsberichte der Berliner
Akademie, http://www.maths.tcd.ie/pub/HistMath/People/Riemann/Zeta/.
Schmitt, Christoph 2010 *Calculation of L-Functions Associated with Newforms: Implementation, Choice of Parameters and Verification of Zeros* http://www.mathematik.uni-wuerzburg.de/~steuding/schmitt.pdf
Silverman J.H. (1986) The Arithmetic of Elliptic Curves, Springer-Verlag.
Silverman J.H. (1994) Advanced Topics in the Arithmetic of Elliptic Curves, Springer-Verlag.
Stein W. (2007) Modular forms, a computational approach, (appendix P. E. Gunnells), Grad. Studies in Math., vol. 79,

Amer. Math. Soc., Providence, RI, 2007. MR 2289048 (2008d:11037) http://modular.math.washington.edu/books/modform/modform/index.html

Stein W. (2008) *An introduction to computing modular forms using modular symbols* Algorithmic Number Theory MSRI Publications 44 http://www.math.leidenuniv.nl/~psh/ANTproc/20stein.pdf

Tate J.C. (1974) *The Arithmetic of Elliptic Curves* lnventiones math. 23, 179-206

Titchmarsh, E. C. (1986) The theory of the Riemann zeta-function, 2nd edition, The Clarendon Press, Oxford Univ. Press, New York Ch X, 10.25

Weil, André (1948), *Sur les courbes algébriques et les variétés qui s'en déduisent, Actualités* Sci. Ind., no. 1041 = Publ. Inst. Math. Univ. Strasbourg 7 (1945), Hermann et Cie., Paris, MR0027151key

Wiles, Andrew (1995), *Modular elliptic curves and Fermat's last theorem*, Annals of Mathematics. Second Series 141 (3): 443–551, ISSN 0003-486X, MR1333035